TECHNISCHE UNIVERSITÄT MÜNCHEN

Fakultät für Medizin

Institut für Mikrobiologie, Immunologie und Hygiene

Stochastic differentiation of single CD4$^+$ T cells is modulated by T cell receptor avidity

Yi-Li Cho

Vollständiger Abdruck der von der Fakultät für Medizin der Technischen Universität München zur Erlangung des akademischen Grades eines

Doctor of Philosophy (Ph.D.)

genehmigten Dissertation.

Vorsitzende/r: Prof. Dr. Roland M. Schmid

Betreuer/in: Prof. Dr. Dirk Busch

Prüfer der Dissertation: 1. Prof. Dr. Thomas Korn

2. Prof. Dr. Percy A. Knolle

Die Dissertation wurde am 21.07.2016 bei der Fakultät für Medizin der Technischen Universität München eingereicht und durch die Fakultät für Medizin am 05.09.2016 angenommen.

Table of Contents

Table of Figures

Abbreviation

ACT	Ammonium-Tris buffer
APC	Antigen presenting cells
APC	Allophycocyanin
APCeF780	Allophycocyanin-eFluor780
APL	Altered Peptide Ligand
BSA	Bovine serum albumin
Bcl-6	B-cell Lymphoma 6
BrdU	5-Bromo-2'-Deoxyuriding
CD	Cluster of differentiation
CCR7	Chemokine receptor 7
CXCR5	C-X-C Motif Chemokine receptor type 5
DC	Dendritic cell
DMSO	Dimethyl sulfoxide
EDTA	Ethylendiaminetetraacetatic acid
EMA	Ethidum monoazide, bromide
eF450	eFluor450
FACS	Fluorescence activated cell sorting
Fc	Fragment crystallizable part
FCS	Fetal calf serum
FITC	Fluorescein-isothiocyanat
Foxp3	Forkhead box P3
GATA3	GATA binding protein 3
GC	Germinal center
IFN-γ	Interferon gamma
IL	Interleukin
Ig	Immunoglobulin
i.p.	intraperitoneal
i.v.	intravenous
KO	Knockout
MHCII	Major histocompatibility complex II
MVA	Modified Vaccinia virus Ankara

OVA	Ovalbumin
PBS	Phosphate buffer saline
PD-1	Programmed death-1
PE	Phycoerythrin
PECy7	Phycoerythrin-Cy7
PerCPCy5.5	Peridinin-chlorophyll proteins-Cy5.5
PI	Propidium iodide
PMA	Phorbol-myristate-acetate
p:MHC	peptide:MHC
Rag1	Recombination activating gene 1
RORγt	RAR-related orphan receptor gamma
RPMI-1640	Roswell Park Memorial Institute-1640
rpm	revolutions per minute
SEM	Standard error of mean
SPF	Specific pathogen free
STAT	Singling transducer and activator of transcription
s.c.	subcutaneous
TEF	T Effector Helper cell
TCMp	T Central Memory precursor cell
TCR	T cell receptor
TFH	T Follicular Helper cell
TGF-b	Transforming growth factor-b
TH	T Helper cell
T-bet	T-box transcription factor
Tn	naive T cell
Treg	regulatory T cell
WT	Wild type

1. Introduction

1.1 $CD4^+$ T cells in immunity

Upon microbial infection $CD4^+$ T cells play an important role in orchestrating the adaptive immune response against various pathogens. $CD4^+$ T cells induce the recruitment of granulocytes or macrophages, support B cell maturation and antibody class switching, and also help the generation of $CD8^+$ memory T cells. Furthermore, they balance the magnitude of immune responses via regulatory mechanisms. In order to initiate this sequence of events, naïve $CD4^+$ T cells, which express lymph node homing receptor L-selectin (CD62L) and chemokine receptor CCR7, must migrate from the blood stream into lymph nodes through high endothelial venules (HEV). In lymph nodes or other secondary lymphatic organs such as the spleen, naïve T cells interact with antigen-presenting cells (APCs) that transmit the dual signal required for $CD4^+$ T cell activation. Professional APCs, process antigen that they have previously taken up in the periphery and present it as peptide fragments bound to their major histocompatibility complex (MHC) molecules I or II. Peptide ligands bound to MHCII (p:MHCII) are presented to $CD4^+$ T cells. The dual signal transmitted by APCs to $CD4^+$ T cells consists of the specific binging of a given TCR to its cognate p:MHCII (signal 1) and the interaction of CD28 expressed on naïve $CD4^+$ T cells with co-stimulatory molecules CD80 and CD86 expressed on APCs (signal 2) (1). Following acquisition of these signals, activated $CD4^+$ T cells will undergo strong proliferation and in parallel differentiate into distinct effector $CD4^+$ T cell subsets. This differentiation process is substantially influenced by cytokines produced by the APC and other leukocytes present in the vicinity of the activated T cells (signal 3). Importantly, naïve $CD4^+$ T cells that receive only signal 1, 2 or 3 from an APC will not be activated. In fact, naïve $CD4^+$ T cells that receive signal 1 alone will even be driven into an inactive state, referred to as anergy. Once T cells are anergic they cannot be activated even in the presence of signal 1 and 2 (2). To achieve an effective activation of naïve $CD4^+$ T cells, it requires good coordination of these three signals in order to guarantee antigen specificity, stabilize the immunological synapse, and induce effector $CD4^+$ T cell subsets that are optimally suited for fighting the invading pathogen.

1.1.1 Clonal selection from the naïve T cell receptor (TCR) repertoire

A diverse TCR repertoire, encompassing TCRs specific for a broad range of pathogen-associated epitopes, is key for providing immune protection to the host. In order to establish this diverse naïve TCR repertoire, *Tcra* and *Tcrb* genes are rearranged by random assembly of variable (V), diversity (D) and joining (J) segments. Rearranged TCRs expressed by developing Thymocytes are then tested for reactivity against self-peptides presented on MHCI and MHCII molecules. During positive thymic selection only T cells expressing TCRs that bind with sufficient avidity to self-p:MHC ligands receive a survival signal (3). This is followed by negative selection, during which those positively-selected T cells that are strongly self-reactive will be signaled to undergo apoptosis (4). Together positive and negative selection, ensure that the TCR repertoire fits to the MHC alleles of the host (thereby establishing 'MHC restriction') and contains as few self-reactive receptors as possible (thereby establishing 'central tolerance'). When a mature $CD4^+$ T cell, carrying a specific TCR that recognizes a particular foreign peptide loaded on the MHCII complex, is recruited in a secondary lymphoid organ and proliferates. In parallel to this clonal expansion, differentiation into long-lived memory and various effector T cell subsets occurs. Depending on which $CD4^+$ T cell subsets are induced, the immune response is modulated to optimally protect against viruses, intra- or extracellular bacteria, fungi or parasites – or it is suppressed by the activity of regulatory T (Treg) cells.

1.1.2 Immune function of $CD4^+$ T cells

$CD4^+$ T cells are also referred to as Helper T cells. They influence the course of immune responses by helping B cells to produce antibody and undergo class switching to defined antibody isotypes. They also interact with various cell types belonging to the innate immune system and enhance their functionality or guide their migratory activity. Due to these activities they serve as key mediators that orchestrate protective immune responses. They help to coordinate the different branches of the immune system and tailor their actions to optimally fight the invading pathogen. In the course of infection, microbial pathogens give rise to the introduction of particular epitopes and induce a characteristic cytokine milieu. $CD4^+$ T cells specific to the relevant peptides are selected in the secondary lymphoid organs and induced to proliferate. In parallel, the specific cytokine milieu influences their differentiation into distinct T helper subsets. Intracellular pathogens

such as mycobacteria or viruses that are recognized and engulfed by macrophages elicit an inflammatory microenvironment, recruit naïve $CD4^+$ T cells to travel to the site of infection, and direct generation of T Helper 1 (TH1) cells. In return, TH1 cells secrete a large amount of interferon (IFN)-γ to increase the microbicidal activity of macrophages and also activate cytotoxic T cells to eradicate intracellular pathogens via induction of apoptosis in the host cells. Infection with eukaryotic parasites induces a differentiation of another T Helper subset better suited to fighting this type of pathogen. This T Helper subset is referred to as TH2. TH2 cells provide support to antibody generation of B cells and direct class switching to isotypes such as IgG1 or IgE (5). IgE secretion supports mast cells in controlling dissemination of parasites (6). However, the effector mechanisms activated by TH2 cells also play a key role in the induction and maintenance of asthma and other allergic disorders (6). Infections with extracellular bacteria and fungi induce yet another type of TH subset that has been termed TH17. It has been found that TH17 cells help to control such infections by stimulating granulopoiesis in the bone marrow and chemotaxis of mature granulocytes to the site of infection (7). These processes are induced by Interleukin (IL)-17 and IL-22 cytokines produced by TH17 cells. These cytokines act in part via activating epithelial cells, as well as the mucosal fibroblasts to produce a chemotactic environment ideal for granulocyte infiltration into the sub-epithelial compartments of the body (8). Consequently, the TH17 cell subset plays a pivotal role in providing immunity in barrier organs such as the gut or the skin. Apart from helping innate immune cells that mediate phagocytosis or fulfill other micobicidal functions, T Helper cells also support and modulate the antibody production of B cells. One of the major functions of $CD4^+$ T cells is to help B cells produce high-affinity antibodies. Affinity maturation of antibodies takes place in a specialized microenvironment within secondary lymphoid organs called the germinal center (GC). GCs are located within B cell follicles and enable the close interaction of B cells with their cognate antigen. The relevant antigens are bound in the form of immune complexes to Fc receptors or complement receptors on the surface of follicular dendritic cells (FDCs) that reside only in B cell follicles. In the germinal center, B cells undergo somatic hypermutation of the DNA segments encoding the antigen-binding regions of their B cell receptor (BCR). In a subsequent selection process, the B cells compete with their newly generated BCRs for binding to their cognate antigen available on FDCs. $CD4^+$ T cells are critical for supporting the survival of those B cells that harbor BCRs of highest affinity to the cognate antigen and thereby, critically support the affinity maturation of the BCR. The Chemokine ligand CXCL13, is secreted by B cells, and is

required for CXC chemokine receptor 5 (CXCR5) expressing $CD4^+$ T cells to relocate to B cell follicles (9). Such CXCR5 expressing cells are also referred to as T Follicular Helper (TFH) cells (10-12). The colocalization of TFH cells with cognate B cells supports specific high affinity antibody production (13). Aberrant $CD4^+$ T cell responses can lead to immunopathology. For that reason, the immune system has evolved mechanisms to prevent the dysregulation of an immune response. This negative regulation of potentially destructive effector T cells is mediated by $CD4^+$ T regulatory (Treg) cells. Treg cells exert various mechanisms to achieve inhibition of detrimental cellular activities ranging from cell-cell contact to suppressive cytokine secretion (14, 15). Hence, protective pathogen-specific immune responses depend on devoted effector helper T cell lineages, which help B-cells and cells belonging to the innate immune system, and which are under the stringent control of Treg cells.

1.2 Diversification of $CD4^+$ T cell lineages

A variety of helper $CD4^+$ T cell lineages have been identified in recent decades. In 1986, the first pioneer research done by Mosmann & Coffman paved the way to better characterize $CD4^+$ T cells governing diverse immune responses (16). They analyzed $CD4^+$ T cells and recognized that mature $CD4^+$ T cells could be categorized into two distinct clones - selectively expressing IL-2 and IFN-γ as TH1 cells, as opposed to IL-4 producers as TH2 cells. Later on, T-bet and GATA-3 were identified to be the master transcription factors of TH1 cells and TH2 cells, respectively (17, 18). This exemplifies the classification of heterogeneous $CD4^+$ T cell subsets on the basis of subset-specific cytokine profiles and transcription factors. The TH1/TH2 dichotomy has been challenged due to the identification of further $CD4^+$ T cell lineages. A subset harboring regulatory properties was first identified by the constitutively expression of the IL-2 receptor α-chain (CD25) (19). Subsequently, the transcription factor Foxp3 was identified as essential for maintaining the function of T regulatory (Treg) cells (20-22). IL-10 and transforming growth factor (TGF)-β, were identified as signature cytokines of Treg cells that impede effector $CD4^+$ T cell proliferation and the onset of inflammatory diseases (23-25). The loss of function mutation or deletion of the Foxp3 gene has been linked to the murine Scurfy model and to severe autoimmune syndrome in humans termed ‘Immune dysregulation, polyendocrinopathy, enteropathy, X-linked’ (IPEX) which is characterized by hyperproliferation of $CD4^+$ T cells

and lethal autoimmunity (26, 27). A further T cell lineage has been identified in the context of autoimmunity: TH17 cells were defined as a new subset depending on the following cues: they do not secrete TH1 or TH2 signature cytokines IFN-γ or IL-4, which inhibit TH17 differentiation (28, 29). Furthermore, TH17 cells express the distinguishing transcription factor retinoic acid-related orphan receptor-γt (ROR-γt) and produce the pro-inflammatory cytokines IL-17A, IL-17F and IL-22, which are important for fighting infections with fungi and extracellular bacteria. Importantly, cytokines produced by TH17 cells also play a crucial role in the induction of autoimmune diseases such as experimental autoimmune encephalomyelitis (EAE) in mice or multiple sclerosis in humans (30-33). A fifth lineage was identified first in human tonsils and exhibited a characteristic localization within or close to B cell follicles (10-12). Later, it was shown that these T Follicular Helper (TFH) cells support the immunoglobulin production of B cells (13). Differentiation into TFH cells is induced by the lineage-specific transcription factor Bcl-6 and inhibited by Blimp-1. Interestingly, Blimp-1 does not interfere with differentiation into the other effector $CD4^+$ T cell subsets, which hints at an early bi-modal differentiation decision into either TFH or other T Helper cells (34, 35). In addition, IL-21 plays an important role in TFH cell regulation (36). Collectively, these data suggest that T Helper cell differentiation allows for at least five distinct choices: TH1, TH2, TH17, Treg or TFH cell differentiation. These developmental decisions have to be optimally regulated to guarantee for host protection against various pathogens and against autoimmunity.

1.2.1 Cytokines determine $CD4^+$ T cell commitment

As discussed above, cytokines are key environmental factors modulating the differentiation of $CD4^+$ T cell subsets (Fig 1). The first striking discovery of cytokine influence on $CD4^+$ T cell development was achieved by an *in vitro* culture system. The addition of IL-4 alone or together with IL-2 into $CD4^+$ T cell cultures boosts TH2 signature cytokine IL-4 secretion through a positive feedback loop and prevents $CD4^+$ T cell commitment into another subset via antagonistic control. Thus, $CD4^+$ T cells producing high levels of IL-4 adopt a TH2 cell fate and suppress IFN-γ production in order to abrogate TH1 cell generation (37, 38). Such positive feedback loops and antagonistic effects of cytokines, have also been found to be a crucial feature for the priming of other Helper T cell lineages. With regard to TH1 cell polarization, IL-12 and IFN-γ secreted by innate immune cells comes into play.

$CD4^+$ T cells co-cultured with macrophages or IL-12 as a supplement show induction of IFN-γ production and down-regulation of IL-4 production (39). In addition, following the establishment of knockout (KO) mouse model, the deficiency of IFN-γ has been shown to produce a pronounced plunge in the expression of the TH1 signature transcription factor, T-bet (40).

The transition from an inflammatory to a tolerogenic environment is induced by the anti-inflammatory cytokine transforming growth factor-β (TGF-β). $CD4^+CD25^-$ naïve T cells are converted into $CD4^+CD25^+$ regulatory T cells through TGF-β signaling: TGF-β initiates Foxp3 expression and converts $CD4^+$ T cells into Treg cells. Treg cells do not proliferate or produce classical effector cytokine like IFN-γ or IL-4 (41). In addition, IL-2 reinforces the expression of Foxp3 in Treg cells together with TGF-β (42). However, TGF-β indeed possesses a versatile function to reciprocally modulate the fate decisions of effector TH17 and Treg cells (43, 44). Surprisingly, TGF-β in co-operation with IL-6 steers naïve $CD4^+$ T cells away from Treg cell development and toward the generation of effector TH17 cells. In line with these findings, IL-6 KO mice show a diminished TH17 cell population and prevalently form regulatory T cells. Yet, simultaneous depletion of the *IL-6* gene and $CD4^+CD25^+$Treg cells restored the establishment of pathogenic TH17 cells. Further research explained that the reason for this is that IL-21 also participates in the regulation of IL-17 and ROR-γt, together with TGF-β but independent of IL-6 (45). Interestingly, the polarization of TFH cells also requires IL-6 and IL-21 cytokines (46, 47). The reports showed that IL-6 and IL-21-deficient mice also displayed a significantly reduced development of TFH cells and GC-B cells.

1.2.2 Intracellular machinery drives $CD4^+$ T cell polarization

Apart from extracellular factors, modulating Helper T cell responses, the signal cascades transmitted by downstream transcription factors also have a significant influence on shaping T cell fate. Signal transducer and activator of transcription (STAT) proteins and other transcription factors that mediate signal received via cytokine receptors, are key factors for lineage specification of TH cells. For instance, IFN-γ activates STAT1 expression followed by induction of T-bet. T-bet augments IFN-γ secretion and thereby starts a positive feedback loop inducing large amount of IFN-γ production, reinforced T-bet expression an stable TH1 polarization *in vitro (48)*. STAT4 proteins are indispensable for

the activity of IL-12-mediated IFN-γ secretion (49, 50). As to TH2 cell commitment, depletion of the *Stat6* gene abrogates IL-4-evoked TH2 responses, which dramatically curtails antibody production (51, 52). Aforementioned Treg and TH17 cell differentiation is tightly regulated by TGF-β and IL-6/IL-21 cytokines. To ensure TH17 commitment, IL-6 initiates the subsequent production of IL-21, resulting in up-regulation of STAT3 proteins. Furthermore, STAT3 augments induction of IL-17 and IL-21 production and expression of the ROR-γt transcription factor. Counteracting this process, IL-2 signaling promotes activation of both STAT5 isoforms, STAT5a and STAT5b, in order to prevent TH17 cell differentiation and stabilize the expression of CD25 and the *foxp3* gene which preserves Treg cell phenotype (53-55). Therefore, the STAT family proteins in collaboration with lineage-specific transcription factors constitute a complex signaling network that secures the generation of the desired $CD4^+$ T cell lineage. Further transcription factors interplay with the aforementioned cytosolic signaling components. The proto-oncogene c-Maf positively modulates IL-4 production and impairs differentiation along the TH1 pathway (56, 57). Additionally, the Runt-related transcription factors (Runx) family, Runx1 and Runx3, respectively program TH17 and TH1 differentiation. Overexpression of the *Runx1* gene enhances IL-17A, IL-17F and ROR-γt expression and thereby skews responses toward TH17 cell development (58). Runx3 is preferentially expressed in TH1 cells and cooperates with T-bet in binding of the *Ifng* promoter and *Il-4* silencer (59). Interestingly, the interferon-regulatory factor (IRF) family has been shown to modulate TH differentiation as well: *IRF1* as a transcriptional target of Stat1 has a bi-functional role with respect to TH1 polarization. A defective *Irf1* gene leads to an increase in IL-4 production and abolishes secretion of IL-12 and IL-23 by APCs. In addition, another member of this family, IRF-4, forms heterodimers with STAT6, which then induces *Gata3* expression and an increase of IL-4 secretion (60). In summary, interplay between cytosolic factors effects the fine-tuning of the complicated regulatory processes that generate a functionally diverse $CD4^+$ T cell response.

1.3 Differences in TCR signal strength affect differentiation of $CD4^+$ T cells

The development of $CD4^+$ T cell subsets is dependent on acquisition of three main signals: Signal 1 is transmitted through binding of a TCR to its cognate p:MHCII ligand presented

on an APC. Signal 2 is transmitted through ligation of co-stimulatory receptors, and signal 3 is induced by recognition of defined cytokines or other soluble factors. The integration of these signals by naïve $CD4^+$ T cells then results in maturation of specific effector TH cells whose function is tailored to the type of invading pathogen. Studies have shown that the engagement of the TCR and p:MHCII complex happens during the initial two days of infection (61). Classically the TCR p:MHCII interaction is considered to function as a switch that sets of the proliferation of activated $CD4^+$ T cells while polarizing cytokines orchestrate their differentiation into various effector subsets such as TH1, TH2, TH17 and TFH cells as well as induced regulatory T (iTreg) cells. However, it has become increasingly clear that the strength of TCR signaling also plays a substantial role in determining the burst size and subset composition of a $CD4^+$ T cell immune response (62). Early studies have focused on investigating the role of TCR signal strength on the differentiation of naïve $CD4^+$ T cells into TH1 or TH2 effector subsets. These studies showed that stronger TCR signaling favored the differentiation of TH1 cells and weaker signaling induced the development of TH2 cells (63, 64). Signal strength was found to be modulated by two factors: 1) the amount of peptide added to T cell cultures leading to high or low densities of p:MHCII on the surface of APCs and long or short duration of antigen presentation (63) 2) the avidity of the molecular interaction between a given TCR and its cognate p:MHCII ligand (65). Some authors refer to these two factors as the “quantity” and “quality” of TCR signaling (66). Later studies have suggested that not only differentiation into TH1 and TH2 cells but also into TH17 and iTreg cells are influenced by these two aspects of TCR signal strength (67).

1.3.1 Effects of TCR signal quantity on $CD4^+$ T cell differentiation

Naïve $CD4^+$ T cells enter lymph nodes from the blood stream and migrate throughout the T cell areas scanning thousands of APCs for the presence of their cognate p:MHCII ligand. There migration throughout the lymphoid tissue is largely congruent with a random walk model. It has been revealed that crawling $CD4^+$ T cells present independent and undirected movement to overcome spatial obstacles, built up by the fibroblastic reticular cell matrix in lymphoid organs (68, 69). The dense stromal cell networks formed within the vicinity of HEVs, which serve as point of entry for naïve $CD4^+$ T cell into lymph nodes, provide an ideal environment for scanning a large number of APCs. Many studies have

been dedicated to characterizing the relationship of ligand density to TCR signal quantity. As mentioned above, early studies have shown that p:MHCII density influences the bifurcate fate decisions of $CD4^+$ T cells into TH1 versus TH2 cells. In these reports, high antigen doses preferentially induced IFN-γ-producing TH1 cells while low doses induce TH2 cell (63, 64). Further study compared the amount of antigen required to induce TH17 cells. The results indicated that TH1 cells are in need of a high dose of peptide, followed by TH17 cells, and TH2 cells at the lowest end (70). Within 1-3 days after initial antigen contact activated $CD4^+$ T cells have been found to migrate to the interface of the T and B cell zone. Here, B cells and $CD4^+$ T cells must interact to fully develop into antibody producing, class-switched B cells and fully differentiated TFH cells (71). Interestingly, prolonged cell-cell contact between T cells and B cells, as well as particularly strong TCR signaling appears to be required for TFH cell differentiation. Moreover, TFH cells seem to not only require such strong TCR signals but are also less susceptible to activation induced cell death normally associated with very strong TCR signaling (72). Further on, the development of Th17 vs. iTreg cells is also influenced by the strength of TCR signaling. Previous studies demonstrated that low-dose antigen exposure enables the maintenance of Treg cell expansion and Foxp3 gene expression both in humans and mice. Furthermore, the Treg cell mediated suppression is more effective in the presence of low antigen doses (73-75). Taken together, $CD4^+$ T cell fate is substantially influenced not only by cytokine-mediated polarizing signals but also by the quantity of TCR signaling – as determined by peptide dose, p:MHCII density and duration of antigen presentation.

1.3.2 Effects of TCR signal quality on $CD4^+$ T cell differentiation

The above-mentioned factors may vary depending on the time and place were a naïve T cell first interacts with its cognate antigen: One APC may have a substantially higher density of cognate p:MHCII ligands on its surface than another. A T cell encountering its antigen in a lymph node far away from the infection site may receive efficient antigen presentation for a much longer period of time than another T cell encountering its antigen directly in the draining lymph node. However, the quality of TCR signaling, as determined by the avidity of the molecular interaction between a given TCR and it cognate p:MHCII ligand, is mainly dependent on the sequence of a T cell's TCR. Thus, it has been argued that naïve $CD4^+$ T cells outfitted with antigen specific TCRs derived from a polyclonal

repertoire will be pre-determined to receive a certain quality of TCR signaling in the event of antigen exposure (76). Until recently, the role of the structural avidity of the TCR:pMHCII interaction has been mainly studied by investigating the responses of naïve T cell populations. The most widely applied tool is to simplify the system by using transgenic $CD4^+$ T cells recognizing one specific epitope with a defined TCR avidity, or to apply Altered Peptide Ligands (APLs), which bind to the same TCR with distinct avidity. An early study by Pfeiffer *et al.* using the APL approach indicated that low-avidity ligands preferentially prime TH2 differentiation (77). Further research showed that native moth cytochrome c (MCC) is prone to induce TH1 cell development, while the APL derivative K99R, mainly leads to TH2 cell induction (65). In order to more precisely address this question, the application of the PCC/MCC specific 5C.C7 TCR and low-avidity 2B4 TCR have been implemented (78). $CD4^+$ T cells expressing the high-avidity 5C.C7 TCR generate a greater number of TFH cells in comparison to those expressing the low-avidity 2B4 TCR (79). Importantly, these observations have been supported by data gathered in a non-transgenic system. Here, high-avidity $CD4^+$ T cells were removed from an endogenous epitope-specific population of naïve T cells by a tetramer-based approach. Interestingly, immune responses derived from the remaining low-avidity epitope-specific population were biased towards TH2 differentiation while the depleted population generated mainly TH1 cells (80). Further studies have suggested that iTreg cell development is differentially modulated by quantity and quality of TCR signaling. While high doses of high avidity peptide have been shown to interfere with iTreg differentiation, low doses of a high avidity peptide appear to induce more stable iTreg development than high doses of a low-avidity peptide (81). Taken together, the quality of TCR signaling seems to play an important role for $CD4^+$ T cell differentiation. Whether the TCR avidity exerts a specific influence on TH differentiation that is distinct from the effects of peptide dose or density remains to be determined. Further on, it remains a challenging question to answer, how strong the influence of TCR avidity is on the differentiation of individual T cells present in a polyclonal TCR repertoire.

1.4 Single $CD4^+$ T cell fate

A wealth of data concerning $CD4^+$ T cell development has been gathered by monitoring immune response derived from mono- or polyclonal *populations* of naïve T cells. However, these studies do not answer how individual epitope-specific $CD4^+$ T cells outfitted with

unique TCRs respond to their cognate peptide, when this peptide is presented on APCs at different densities, for different periods of time and in the context of varying costimulatory and cytokine-derived signals. In order to understand how TCR avidity to p:MHCII influences responses that originate under these conditions, one must follow the fate of an individual naïve T cell and its progeny *in vivo*. Recently, such single cell approaches have been pioneered for $CD8^+$ T cells (82-86). Two main strategies for single cell fate mapping were used in these studies – genetic barcoding and single cell transfer of T cells harvested from various congenic mouse strains. Both strategies aim at introducing heritable labels that identify a single cell and all of its progeny *in vivo*. The two strategies both rely on TCR-transgenic T cells as a source for the transferred T cells and differ mainly in how the uniqueness of the introduced labels is ensured. Cellular barcoding guarantees uniqueness through providing a sufficient amount of cellular barcodes. These are introduced via retroviral transduction either directly into T cells (87) or into developing Thymocytes (83, 85). Since retroviral transduction requires activation of T cells, only the latter method allows for generating naïve barcoded T cells. Following reintroduction of transduced Thymocytes via intrathymic injection, naïve barcoded $CD8^+$ T cells can be harvested from the secondary lymphoid organs 2-4 weeks later. Barcoded T cells also carry a fluorescent label (e.g. GFP) that allows for sorting these cells and transferring them into tertiary recipients, in which the actual immunological experiment is conducted.

Single cell adoptive transfer of congenic T cells relies first on generating congenic donor strains that harbor the transgenic TCR of interest and one of eight unique combinations of congenic markers CD45.1/.2 and CD90.1./.2 (84). These congenic markers are heritable and allow for discerning adoptively transferred cells from host cells. Importantly, congenic markers are generally considered as a non-immunogenic label and thus do not entail the risk of leading to rejection of transferred T cells. To ensure that every transferred T cell carries a unique label T cells are sorted individually from eight congenic donors and then transferred as an “8x1” cell transfer. This approach is the only one that allows to directly control the single cell origin of the observed T cell responses.

By using a limiting dilution approach single cell fate mapping has also been attempted for $CD4^+$ T cells (88, 89). In contrast to the above-mentioned studies, this approach does not rely on TCR-transgenic donors. Instead, naïve $CD4^+$ T cells specific to a defined epitope are enriched by use of suitable p:MHCII tetramers coupled to magnetic beads. Magnetic enrichment allows for harvesting these very rare cells and then for measuring their frequency in the enriched fraction via flow cytometry. Once the average frequency of naïve

epitope-specific T cells within a given mouse strain is determined, enrichment is performed from another donor mouse belonging to the same strain. The enriched cell fraction is diluted and adoptively transferred to naïve secondary hosts. To determine how much a sample needs to be diluted, it is assumed that progeny will only be recovered from 10% of adoptively transferred T cells (88). These values are mainly based on estimates previously inferred from adoptive transfer of T cell populations (90). While providing access to endogenous T cells, these limiting dilution studies harbor considerable uncertainty as to the true single cell origin of the immune responses monitored (91). Despite its technical limitations this approach has provided exiting insights into immune responses against *Listeria monocytogenes* (L.m.) derived from very low numbers of endogenous epitope-specific T cells. It was demonstrated that $CD4^+$ T cells derived from a polyclonal repertoire generated highly variable responses when these originate from or close to the single cell level. Such responses showed strong biases towards TH1, TFH or germinal center TFH (GC-TFH) differentiation. Nonetheless, the average response derived from populations of polyclonal $CD4^+$ T cells showed a characteristic differentiation pattern (88). These data were interpreted as an indication that distinct TCR avidities determine distinct differentiation patterns derived from single $CD4^+$ T cells. However, this assumption was not directly tested. Thus, it remains incompletely understood in how far TCR avidity really shapes the fate decisions of individual epitope-specific $CD4^+$ T cells.

2. Thesis objectives

The individual $CD4^+$ T cells constituting an epitope-specific population have been suggested to each express a unique TCR that binds with distinct avidity to the relevant p:MHCII (88). Consistent with the pivotal role of TCR signaling for T cell activation, it has been shown that the proliferation and differentiation pattern of a $CD4^+$ T cell population is controlled by TCR avidity (65, 79, 80, 92). However, it remains incompletely understood how this deterministic impact of TCR avidity, perceived on the population level, emerges out of the fate decisions of individual epitope-specific T cells as they proliferate and differentiate within the complex environment of an ongoing infection or vaccination.
The objective of this thesis was to investigate this question and provide a better understanding of how TCR avidity influences the fate of individual $CD4^+$ T cells and their progeny *in vivo*.

The detailed aims of this thesis were:

1) To perform a detailed phenotypic and functional characterization of a monoclonal population of T cells responding to vaccination with a strongly binding cognate peptide and a weakly binding Altered Peptide Ligand.
2) To generate eight congenic donor strains expressing the same TCR transgene on a Rag1-competent and a $Rag1^{-/-}$ background.
3) To perform single T cell fate mapping experiments by utilizing these congenic strains for single cell adoptive transfer experiments.
4) To identify the lineage relationships between long- and short-lived $CD4^+$ T cells based on these single cell-derived data and supported by computational modeling.
5) To validate the predicted lineage relationships by performing suitable experiments on population level.

3. Materials and Methods

3.1 Materials

3.1.1 Chemicals and Reagents

Chemicals/Reagents	Provider
Ammonium chloride (NH_4Cl)	Sigma, Taufkirchen, Germany
Albumin from chicken egg white	Sigma, Taufkirchen, Germany
Bovine serum albumin (BSA)	GE Healthcare, Munich, Germany
BrdU kit	BD Biosciences, Heidelberg, Germany
Brefeldin A (Golgi Plug)	BD Biosciences, Heidelberg, Germany
Complete Freund's Adjuvant	Sigma, Taufkirchen, Germany
Cytofix/Cytoperm	BD Biosciences, Heidelberg, Germany
DNase I	Sigma, Taufkirchen, Germany
Ethanol	Klinikum rechts der Isar, Munich, Germany
Ethidium-monoazide-bromide (EMA)	Molecular Probes, Leiden, the Netherlands
Ethylenediaminetetraacetic acid (EDTA)	Roth, Kalsruhe, Germany
Feel calf serum (FCS)	Biochrom, Berlin, Germany
Fixation viability dye eFlour 780	eBioscience, San Diego, California, US
Foxp3 Staining Buffer Set	eBioscience, San Diego, California, US
Golgi-Plug	BD Biosciences, Heidelberg, Germany
Heparin-Natrium-25000	Ratiopharm, Ulm, Germany
Hydrochloride (HCl)	Roth, Kalsruhe, Germany
Ionomycin	Sigma, Taufkirchen, Germany
Magnesium chloride ($MgCl_2$)	Sigma, Taufkirchen, Germany

Phorbol-myristate-acetate (PMA)	Sigma, Taufkirchen, Germany
Phospate buffered saline (PBS)	Biochrom, Berlin, Germany
Propidium iodide (PI)	Invitrogen, Carlsbad, CA, USA
RPMI 1640	PAA Laboratories, Pasching, Austria
Sodium azide (NaN3)	Sigma, Taufkirchen, Germany
Sodium chloride (NaCl)	Roth, Kalsruhe, Germany
Sodium hydroxide (NaOH)	Roth, Kalsruhe, Germany
Streptavidin PE	BD Pharmingen, San Diego, USA
Streptavidin PE	eBioscience, San Diego, California, USA
Streptavidin PE	Biolegend, San Diego, California, USA
Trypan Blue	Sigma, Taufkirchen, Germany
Gibco® RPMI 1640 medium	PAA, Pasching, Austria

3.1.2 Antibodies (Mouse)

Antibodies	Fluorochromes	Clones	Provider
αBcl-6	PE-Cy7	K112-91	BD Biosciences, Heidelberg, Germany
αBrdU	FITC	PRB-1	eBioscience, San Diego, California, USA
αBrdU	FITC	Bu20a	eBioscience, San Diego, California, USA
αCD16/32 (Fcγ-RII/III)		2.4G2	BD Biosciences, Heidelberg, Germany
αCD19	PE-CF594	1D3	BD Biosciences, Heidelberg, Germany
αCD25	APC	PC61	BD Biosciences, Heidelberg, Germany
αCD27	PE	LG.7F9	eBioscience, San Diego, California, USA
αCD27	APC	LG.7F9	eBioscience, San Diego, California, USA
αCD3	PE-Cy7	145-2C11	eBioscience, San Diego, California, USA
αCD4	FITC	RM4-5	eBioscience, San Diego, California, USA

αCD4	PE	H129.19	BD Biosciences, Heidelberg, Germany
αCD4	PerCP-Cy5.5	RM4-5	eBioscience, San Diego, California, USA
αCD4	eF450	RM4-5	eBioscience, San Diego, California, USA
αCD4	Pacific Orange	RM4-5	Invitrogen, Carlsbad, CA, USA
αCD4	APC	GK1.5	eBioscience, San Diego, California, USA
αCD44	FITC	IM7	eBioscience, San Diego, California, USA
αCD44	APC	IM4	eBioscience, San Diego, California, USA
αCD45.1	FITC	A20	eBioscience, San Diego, California, USA
αCD45.1	PerCP-Cy5.5	A20	eBioscience, San Diego, California, USA
αCD45.1	eF450	A20	eBioscience, San Diego, California, USA
αCD45.1	APC	A20	eBioscience, San Diego, California, USA
αCD45.2	FITC	104	eBioscience, San Diego, California, USA
αCD45.2	Horizon V450	104	BD Biosciences, Heidelberg, Germany
αCD62L	FITC	MEL-14	BD Biosciences, Heidelberg, Germany
αCD62L	PE-Cy7	MEL-14	eBioscience, San Diego, California, USA
αCD90.1	FITC	OX7	BD Biosciences, Heidelberg, Germany
αCD90.1	PE	HIS51	eBioscience, San Diego, California, USA
αCD90.1	APC	HIS51	eBioscience, San Diego, California, USA
αCD90.1	APCeF780	HIS51	eBioscience, San Diego, California, USA
αCD90.2	APC	53.2.1	eBioscience, San Diego, California, USA
αCD90.2	APCeF780	53.2.1	eBioscience, San Diego, California, USA
αCXCR5	PE	SPRCL5	eBioscience, San Diego, California, USA
αFoxp3	eF450	FJK16s	eBioscience, San Diego, California, USA
αGATA3	PE-Cy7	TWAJ	eBioscience, San Diego, California, USA
αIFN-γ	PE-Cy7	XMG1.2	eBioscience, San Diego, California, USA
αIL-2	PE	JES6-5H4	eBioscience, San Diego, California, USA
αPD-1	PE-Cy7	J43	eBioscience, San Diego, California, USA

αPE	Biotin	eBioPE-DLF	eBioscience, San Diego, California, USA
αRORγt	APC	B2D	eBioscience, San Diego, California, USA
αT-bet	BV421	Apr46	BD Biosciences, Heidelberg, Germany

3.1.3 Buffers

Buffers	Recipe	
Ammonium chloride-Tris (ACT)	0.17 M	NH_4Cl
	0.3 M	Tris-HCl, pH 7.5
DNase-I-Puffer	75ml	NaCl
	in 50% (v/v)	Glycerol
FACS buffer	1x	PBS, pH 7.5
	0.5% (w/v)	BSA
	2mM	EDTA
RP10+-cell culture medium	1x	RPMI-1640
	10% (v/v)	FCS

3.1.4 Peptides

Peptides	Sequences	Suppliers
$OVA_{323-339}$ (OVA_{WT}) in NaCl solution	ISQAVHAA**H**AEINEAGR	Peptide & Elephant, Postdam, Munich
OVA_{R331} in NaCl solution	ISQAVHAA**R**AEINEAGR	Peptide & Elephant, Postdam, Munich

3.1.5 Equipment

Equipment	Model	Provider
Cytometer	Cyan ADP Analyser	Beckman Coulter, Fullerton, California, US
	MoFlo Legacy Cell Sorter	Beckman Coulter, Fullerton, California, US
	FACSAria III Cell Sorter	BD Biosciences, Heidelberg, Germany
Centrifuge	Biofuge fresco	Heraeus, Hanau, Germany
	Multifuge 3 S-R	Heraeus, Hanau, Germany
	Sorvall® RC 26 Plus	Heraeus, Hanau, Germany
	Varifuge 3.0RS	Heraeus, Hanau, Germany
	Biofuge stratos	Heraeus, Hanau, Germany
Incubator	Cytoperm 2	Heraeus, Hanau, Germany
	Minitron	Infors, Bottmingen, Switzerland
	BE 500	Memmert, Schwabach, Germany
BioSafety Cabinets	HERAsafe	Heraeus, Hanau, Germany
Hemocytometer	Neubauer	Schubert, Munich, Germany
Water Bath	LAUDA ecoline 019	Lauda, Königshofen, Germany
pH-meter	MultiCal® pH 526	WTW, Weilheim, Germany
Weighing Scale	CP 124 S	Sartorius, Göttingen, Germany

3.1.6 Software

Software	Provider
Adobe Illustrator	Adobe Systems, San Jose, USA
EndNote Program	Microsoft, Redmond, USA
FlowJo	Treestar, Ashland, USA
FACS Diva	BD Biosciences, Heidelberg, Germany
Graphpad Prism	Graph Pad Software, La Jolla, USA
Microsoft Office	Microsoft, Redmond, USA
Summit V4.5	Beckman Coulter, Fullerton, California, US

3.2 Methods

3.2.1 Mice and peptide immunization

Six- to eight- week-old C57BL/6 female mice were purchased from Harlan (now Envigo). OTII and OTII Rag1$^{-/-}$ mice expressing eight distinct congenic marker combinations of CD45.1, CD45.2, CD90.1 and CD90.2 were bred in-house at the animal facility of Technische Universität München. Animal care and experiments were in accordance with institutional protocols as approved by the relevant local authorities. For peptide immunization, C57BL/6 mice were injected subcutaneously (s.c.) at the tail-base with 10-100µg OVA_{WT} or OVA_{R331} plus Complete Freund's Adjuvant (CFA).

3.2.2 Adoptive T cell transfer

Naïve CD4^{+}CD25^{-}CD44^{lo} cells were purified from the peripheral blood of eight OTII or OTII Rag1$^{-/-}$ congenic donor mice to >99% purity by flow cytometric cell sorting (MoFlo XDP, Beckman Coulter). Leukocytes from peripheral blood were stained with anti-CD44-FITC (IM4, eBioscience), anti-CD4-eF450 (RM4-5, eBioscience) and anti-CD25-APC (PC61, BD Biosciences) for 20min at 4ºC including propidium iodide (PI) labeling to discriminate live/dead cells. Naïve CD4 cells (1, 10 or 1000 cells) from eight OTII congenic donors were consecutively sorted into the same well of a V-bottom 96-well plate, containing 200µL of heat-inactivated fetal calf serum (FCS) containing 4x10^{5} peripheral blood monocytes from C57BL/6 mice. Afterwards, each well contained of 8x1, 8x10, 8x100, 8x1000 cells with distinct congenic phenotypes that were injected intraperitoneally (i.p.) into C57BL/6 mice.

3.2.3 Flow cytometric analysis

Eight days after OVA_{WT} or OVA_{R331} peptide immunization, lymphocytes were isolated from draining lymph nodes of C57BL/6 mice, and homogenized by mechanical disruption on a sterile 70µm cell strainer in RPMI 1640 medium containing FCS. For antibody staining, 2 x 10^{7} cells were loaded into U-bottom 96-well plates and incubated with anti-CD16/32 (Fc-block; MR9-4, BD Biosciences) for 20 min. Subsequently, CXCR5 staining was performed in three successive steps by using anti-CXCR5-PE (SPRCL5, eBioscience) for 30 min, a secondary biotinylated-anti-PE (eBioPE-DLF, eBioscience) antibody for 20 min and then

with Streptavidin-PE (BD Biosciences) in combination with any of the following labeling matrices: anti-CD45.1-FITC (A20, eBioscience), anti-CD90.1-FITC (OX7, BD Biosciences) or anti-CD62L-FITC (MEL-14, eBioscience), anti-CD19-PE CF594 (1D3, BD Biosciences), anti-CD45.1-PerCP Cy5.5 (A20, eBioscience), anti-CD62L-PE Cy7 (MEL-14, eBioscience) or anti-PD-1-PE Cy7 (J43, eBioscience), anti-CD45.2-Horizon V450 (104, BD Biosciences) or anti-CD45.1-eF450 (A20, eBioscience), anti-CD4-Pacific Orange (RM4-5, Invitrogen), anti-CD90.1-APC (HIS51, eBioscience), anti-CD27-APC (LG.7F9, eBioscience), anti-CXCR3-APC (CXCR3-173, eBioscience) or anti-CD62L-APC (MEL-14, eBioscience) and anti-CD90.2-APCeFluor 780 (53-3.1, eBioscience) for 20min. All staining procedures were performed at room temperature. For intracellular transcription factor staining, cells were first incubated with ethidium monazide (EMA) and Fc block, then subjected to a 3-step CXCR5 staining procedure, as described, followed by staining of the surface markers anti-CD62L-FITC (MEL-14, eBioscience), anti-CD19-PE CF594, anti-CD4-Pacific Orange and anti-CD45.1-APC (A20, eBioscience).

For intracellular cytokine staining of endogenous CD4 T cells, C57BL/6 mice were s.c. immunized with OVA_{WT} or OVA_{R331} peptide, both plus CFA. On day 8 after immunization, 10^7 lymphocytes from dLN were restimulated for 5 hours at 37°C in the presence of DMSO, 1µg OVA_{WT} or 1µg OVA_{R331} peptide, and Brefeldin A (Golgi Plug, BD Biosciences) for the final 3 hours. Cells pre-incubated with EMA and Fc block, were further stained with anti-CD19-PE CF594, anti-CD4-Pacific Orange and anti-CD44-APC (IM4, eBioscience).

In accordance with manufacturer guidelines, intracellular staining with anti-T-bet-BV421 (Apr46, BD Biosciences), anti-RORγt-APC (B2D, eBioscience), anti-Foxp3-eFluor 450 (FJK-16s, eBioscience), anti-GATA3-PE Cy7 (TWAJ, eBioscience), anti-Bcl-6-PE Cy7 (K112-91, BD Biosciences) or anti-IL-2-PE (JES6-5H4, eBioscience) as well as anti-IFN-γ-PE Cy7 (XMG1.2, eBioscience) was done at 4°C for 30 min after fixation and permeabilization.

Measurements were done on a 9-color CyAn ADP Flow Cytometer (Beckman Coulter). Analyses were performed via Summit software (Beckman Coulter) and FlowJo software (TreeStar).

3.2.4 Recall experiments

Initially 10^4 $CD45.1^+$OTII cells were adoptively transferred to primary C57BL/6 recipients, which were subsequently immunized s.c. with OVA_{WT} peptide plus CFA. Lymphocytes

were isolated from lymph nodes, spleen and bone marrow of recipients on day 8 p.i. Flow cytometric cell sorting was used to purify $CXCR5^{-}CD62L^{-}$ TEF cells, $CXCR5^{-}CD62L^{+}$ or $CXCR5^{+}CD62L^{+}$ TCMp cells and $CXCR5^{+}CD62L^{-}$ TFH cells, 5000 cells of these subsets were transfered i.p. into separate naïve recipients. After resting for 35 days in the absence of antigen, mice were recalled by i.v. infection with 10^{8} pfu MVA-OVA or s.c. immunization with OVA_{WT} plus CFA. The response was evaluated on day 8 after recall in spleen or dLNs, respectively.

3.2.5 BrdU incorporation

Mice were administered 1mg bromodexoyuridine (BrdU) i.p. and given 0.8 mg/ml BrdU plus 1mg/ml sucrose in drinking water for one day before analysis. For BrdU analysis, the staining procedures were performed according to the BrdU Flow Kit (BD Biosciences) and included surface marker labeling as indicated above.

3.2.6. General statistical Analysis

Unless indicated statistical significance was determined by one-way ANOVA with Tukey's multiple comparison testing. Asterisks indicate statistical significance * $p<0.05$, ** $p<0.01$ *** $p<0.001$.

3.2.7. Bio-mathematical modeling

Dr. Michael Flossdorf and Professor Thomas Höfer at the DKFZ Heidelberg performed the mathematical modeling. A concise version of the modeling approach is provided here.
The data in Fig. 20 were constructed based on the single cell dataset to simulate population responses. Based on the 4.2% of detectable progenies originating from transferred single cells, each simulation was generated by randomly drawing 42 times from the single cell dataset. The progeny size and phenotype of a population response were constructed by summing the randomly drawn data. The same approach was employed in the probabilistic "Model I" shown in Fig. 21 to simulate single cell behaviors (Fig. 22A). To predict the population-derived response in Fig. 22B, Gillespie's algorithm was additionally included for the formulation. The simulation of population responses

under low-avidity conditions involved the same approach, but with adapted proliferation and differentiation rates as compared to “Model I”.

To construct “Model I” and “Model II”, the rates of proliferation and differentiation were assumed to be in accordance with standard Markov processes and the parameter estimation was performed according to published literature. In brief, we implemented standard χ^2-minimization using summary statistics for the cell numbers of the single-cell derived progenies at day 8 post immunization (data shown in Fig. 20) in the objective function (mean values and coefficients of variation for the CD62L positive and negative subset sizes, Pearson correlation between the subset sizes). Non-parametric bootstrapping was used to assess the uncertainties of those five quantities. The 95% confidence intervals for the prediction bands shown in Fig. 21 were obtained by repeatedly fitting both models to bootstrap samples of the single cell-derived progeny data.

4. Results

4.1 Local $OVA_{323-339}$ peptide immunization induces production of T Effector Helper (TEF) cells, T Central Memory precursor (TCMp) cells and T Follicular Helper (TFH) cells.

C57BL/6 mice received CD45.1-expressing naïve $CD4^+$ T cells from transgenic OTII mice harboring a chicken ovalbumin $OVA_{323-339}$-specific TCR, in combination with immunization with cognate peptide in complete Freund's adjuvant (CFA). CFA, containing paraffin oil and heat-killed Mycobacteria, efficiently generates a local inflammatory response. Therefore, subcutaneous (s.c.) tail-based immunization of $OVA_{323-339}$ (OVA_{WT}) peptide emulsified in the depot-forming adjuvant CFA has the potential to efficiently generate an accumulation of peptide-specific $CD4^+$ T cells in the lymph nodes draining the vaccination site. On day 8 after immunization, these activated $CD4^+$ T cells had differentiated into three distinct subsets discriminated by the expression of CXCR5 and CD62L (Fig. 2A). The chemokine receptor CXCR5 has been shown to be necessary for the migration of Helper T cells and B cells to the B cell follicles in secondary lymphoid organs. Based on their migratory properties $CXCR5^-CD62L^-$ TEF cells (migrating to non-lymphoid organs), $CD62L^+$ T cells (residing in lymphoid nodes) and $CXCR5^+CD62L^-$ TFH cells (residing in close proximity to B cell follicles) can be defined. The lymph node-homing receptor, CD62L, has also been used to describe long-lived central memory T cells, which rapidly proliferate during recall responses against secondary infections. Therefore, we first assessed whether CD62L expression identifies TCM precursor (TCMp) cells already at the peak of the response. Therefore, we sorted TEF and TFH as well as $CXCR5^+$ and $CXCR5^–$ putative TCMp cells on day eight after vaccination via flow cytometry. Subsequently, the sorted cells were separately transferred into naïve secondary hosts. After 35 days, these mice were challenged either with Modified Vaccinia Ankara-OVA (MVA-OVA) virus to elicit a systemic recall response or with OVA_{WT} peptide in CFA to generate a local recall response (Fig. 2A). The desired cell subsets were sorted to high purity (Fig. 2B). We found that TCMp cells, regardless of CXCR5 expression, mount superior secondary responses in both recall schemes in comparison to $CD62L^-$ TEF and TFH subsets (Fig. 2C). Therefore, $CD62L^+$ Helper T cells present at the peak of expansion indeed functioned as TCMp cells. Further analysis of the three defined subsets (Fig. 3A)

for expression of the lineage-specific transcription factors T-bet, GATA3, RORγt, Foxp3 and Bcl-6 provided additional information concerning their molecular makeup (Fig. 3B). $CXCR5^{+}CD62L^{-}$ TFH cells highly expressed Bcl-6, while their TCMp and TEF counterparts displayed only moderate expression of this transcription factor. Remarkably, TEF cell populations express both T-bet and RORγt, which indicates the presence of TH1 and TH17 cells in this compartment. Additionally, in this strongly inflammatory environment, the three cell subsets produce neither GATA3 nor Foxp3, which are the specific transcription factors for TH2 and Treg cells, respectively. This finding is congruent with previous studies demonstrating that the generation of TH2 and Treg cells is correlated to weak stimulatory signals. Hence, the surface markers CXCR5 and CD62L can confidently be applied to evaluate the development of naïve $CD4^{+}$ T cells into epitope-specific TCMp, TEF and TFH cell subsets after peptide vaccination.

4.2 Avidity of TCR-p:MHCII interaction determines burst size and subset composition of population-derived responses.

Polyclonal naïve $CD4^{+}$ T cell populations are composed of diverse T cell clones that can recognize a broad variety of pathogens. The initiation of naïve $CD4^{+}$ T cell activation in order to clear pathogens requires the interaction of a T cell outfitted with an epitope-specific T cell receptor (TCR) and a cognate peptide:MHC class II complex (p:MHCII) expressed on antigen-presenting cells (APCs). It has been proposed that intrinsic TCR avidities play a decisive role in controlling the proliferation and differentiation of epitope-specific $CD4^{+}$ T cells. However, each naïve T cell in the populations which possess the same p:MHCII-specificity express different TCRs that interact with the cognate complex with differing avidities. Thus, it is pertinent to investigate the influence of distinct TCR avidities on the diversity of $CD4^{+}$ T cell repertoires. In order to address this question, we established an OTII congenic matrix mouse model to investigate $CD4^{+}$ T cell responses from multiple donors expressing identical TCRs in the same host. OTII TCR-transgenic mice (expressing CD45.2 and CD90.2) were first bred with CD45.1 or CD90.1 congenic mice to yield offspring possessing a CD45.1/.1, CD45.1/.2, CD45.2/.2 phenotype in combination with CD90.1/.1, CD90.1/.2, CD90.2/.2 congenic backgrounds. Furthermore, they were crossbred to produce eight strains with different combinations of congenic marker expression that are discernable from the host's congenic phenotype. Thereby, we could transfer eight "OTII congenic matrix mice" per recipient mouse in our study. This

multiplexed approach enabled us to simultaneously analyze the fate decisions of these eight OTII T cell populations (Fig. 4). Four fluorescent antibodies directed against CD45.1, CD45.2, CD90.1 and CD90.2 suffice to identify these eight OTII donor strains (Fig. 5).

Altered Peptide Ligands (APLs) have been previously employed to elucidate the impact of TCR-Ligand affinity on the character of $CD4^+$ T cell responses. To this end, we utilized the OVA_{R331} peptide, which is an APL of the OVA_{WT} peptide, in which the amino acid histidine at position 331 is replaced with arginine (Fig. 6A). This results in a low-avidity TCR-p:MCHII interaction (93). We tested the possibility that the alteration of the cognate peptide changes its presentation on the MHCII complex of APCs. To do so, we immunized C57BL/6 mice with either OVA_{WT} or OVA_{R331} peptide emulsified in CFA and analyzed the secretion of the characteristic cytokines IFN-γ and IL-2 from endogenous $CD4^+$ T cells responding to the indicated peptides (Fig. 6B). Collected data revealed that despite the modification in position 331 this APL was still able to induce an effective epitope-specific immune response (Fig. 6C). We then further investigated the cellular response of monoclonal $CD4^+$ T cell populations exposed to OVA_{WT} or OVA_{R331}. 8x1000 OTII congenic donor cells were adoptively transferred into C57BL/6 mice and followed by immunization of either the OVA_{WT} peptide or OVA_{R331} peptide, which possess strong or weak binding strength to the relevant TCR. Descendants of the eight groups of transferred cells induced by these two distinct peptides are capable of being identified in dLNs at the peak expansion (Fig. 7 and 8). Moreover, the population-derived response in both cases represents phenotypic and proliferative homogeneity (Fig. 9A and B). As predicted, high avidity TCR ligation results in a characteristic subset distribution that is dominated by TEF and TFH subsets, with relatively weaker differentiation into TCMp. Weak TCR-p:MCHII interaction reduced the size of expansion by about 11 times and produced an evidently distinct response pattern, which is composed of substantially decreased TFH cell subsets and relatively more TCMp cells. Thus, OVA_{R331} peptide triggers a weaker cellular response, which leads to responding cells expanding less. Considering these factors, we investigated whether a reduced density of OVA_{WT} peptide also directed the response pattern toward that induced by APL OVA_{R331} vaccination. Accordingly, we reduced the given peptide dose of OVA_{WT} by 10-fold, demonstrating that decreasing the p:MHCII density 10-fold does not skew the cellular response toward a low-avidity ligation pattern, but rather that the characteristic phenotype remains constant (Fig. 10).

4.3 Single T cells respond stochastically to high avidity TCR ligation despite harboring identical TCRs.

Based on the observation that TCR avidity is strongly deterministic for population-derived responses, we next studied how this variable impacts on single cell behavior. To this end, single naïve $CD4^+$ T cells were sorted from the peripheral blood of eight OTII congenic donor mice and simultaneously co-transferred into one C57BL/6 mouse (Fig. 11). Single cell sorts and adoptive transfers were performed as previously described (84). After cell transfer, mice were immunized s.c. at the tail base with OVA_{WT} emulsified in CFA. The differentiation pattern of progenies derived from individual $CD4^+$ T cells could be detected in dLN at the peak response (Fig. 12). Importantly, we were able to identify distinct effector cell types from two individual monoclonal $CD4^+$ T cells within the same host (Fig. 12). Further analysis emphasized that single $CD4^+$ T cells harboring an identical TCR showed a strong variation in expansion size and subset composition after undergoing an interaction with high avidity TCR ligation (Fig. 13). The variation may potentially have been due to residual TCR expression in OTII congenic mice. We controlled for expression of such additional TCRs by performing experiments with OTII $Rag1^{-/-}$ donors, which produce only OVA_{WT}-specific TCRs and can not assemble additional endogenous TCRs. Compiled results indicated that the response size of monoclonal single $CD4^+$ T cells varies by about 180-fold when comparing the largest and smallest progeny, which surpasses the difference of immune responses created by high and low avidity TCR-p:MHCII interaction (Fig. 14).

As demonstrated in a previous study, the tetramer-based enrichment followed by a limiting dilution approach has been applied to predict single cell development (88). Accordingly, we extended our research to study the immune response generated from a limiting number of cells. At first, we assessed the recovery rate of the adoptive single T cell transfers performed in our model. The result revealed a 4.2% take rate of detectable progeny derived from single $CD4^+$ donor T cells (Fig. 15A). When the yield of 4.2% detectable progeny in a single T cell transfer is taken into account, the anticipated take rate for 10-, 100- and 1000- T cell transfers would be 34.9%, 98.6% and 100%, respectively. Our titration studies closely matched these expected values, which yielded detectable progeny in 38% of 10-cell transfers and 100% for 100- as well as 1000-cell transfers (Fig. 15B). Further analysis indicated that 10-cell transfers could produce an 80% rate of recovered progeny derived from bona fide single $CD4^+$ T cells (Fig. 16A). These

results were further confirmed by analyzing the response size of 1-, 10-, 100-, and 1000 cell transfers, which showed that 10 precursor cells generated a similar progeny size in relation to those originating from single cells (Fig. 16B). In addition, the fold change of 100- and 1000-cell derived responses is close to the prediction based on a 4.2% take rate.

We then initiated a 10-cell transfer model comprised of monoclonal T cells coupled with the aforementioned vaccination strategy with OVA_{WT} peptide. The 10-cell derived progenies still displayed the immense difference in response size and differentiation pattern shown in the previous single cell study (Fig. 17A and B). Moreover, we wished to assess whether or not the phenotypic disparity is a global trend or simply restricted to the subset discrimination we defined. Therefore, we included another universal surface marker, PD-1, which has been used in combination with the chemokine receptor CXCR5 to identify a specific TFH cell subset localized in the germinal center (GC), a specialized microenvironment where TFH cells help B cell maturation and the production of high affinity antibodies. Use of the CXCR5 and PD-1 markers demonstrated a consistent differentiation pattern that could still be observed on the population level (Fig. 18), but phenotypic heterogeneity was clearly present, exemplified by two 10-cell derived progenies in the same host (Fig. 19). Taken together, the “very low number transfer” model, which is close to the limiting dilution approach, created a great variation in size and effector cell phenotypes, as with single cell strategies. This finding indicated that deterministic TCR properties can predict the population-derived response, but a vast diversity of stochastic factors outperforms the intrinsic TCR influence on single cell behavior.

4.4 TCR avidity modulates the probability of stochastic division and differentiation events.

To gain an in-depth understanding of the relationship between the stochastic heterogeneity of single cell-derived response sizes and differentiation patterns, as well as the rather homogenous, deterministic TCR influence on a population level we employed the use of an unbiased computational system to simulate the $CD4^+$ T cell behavior based on the measured data. The 4.2% take rate of individual $CD4^+$ T cell transfers demonstrates that transferred cells could survive and be detected in our adoptive cell transfer model. Hence, we could expect that by cumulating the data from 42 precursor cells *in vivo*, it would ideally be possible to rebuild the population response pattern generated by 1000

cells. We thus simulated a population response *in silico* via randomly drawing 42 times from the single cell data set. After multiple runs of this approach, we could construct a set of predicted progeny sizes and effector cell types on the population level. Strikingly, the formulated response pattern is closely in line with the population-derived response generated *in vivo* (Fig. 20). The results indicated that at least 42 $CD4^+$ precursor cells are required to achieve an optimally robust response. Also, populations of $CD4^+$ T cells responding to high avidity TCR ligation develop a predictable response pattern while accumulating adequate numbers of monoclonal T cells, while each individual cell could reasonably be expected to experience unpredictable stochastic events which influence its differentiation. Furthermore, we aimed to design a computational model that could predict the behavior of T cells under different conditions. Accordingly, we constructed two dynamic models based on the developmental hierarchy, which hypothesized that naïve $CD4^+$ T cells develop into $CD62L^+$ TCMp cells, then further differentiate to $CD62L^-$ non-TCMp cells or, in reverse, $CD62L^+$ TCMp cells arise from $CD62L^-$ non-TCMp cells (Fig. 21A). We found that only “Model I” could be accurately correlated to the developmental kinetics of $CD4^+$ T cells based on the $CD62L^+$ expression from the early activation phase until peak response phase (Fig. 21B). Subsequently, we simulated the $CD4^+$ T cell response in relationship to progeny size against $CD62L^+$ expression according to Model I. This showed that the modeling data are in good accordance to the measured single $CD4^+$ T cell responses *in vivo* (Fig. 22A). After performing repetitive simulations on an average of 42 runs, the cumulative data from the simulation also mirrored the population-derived response (Fig. 22B). Moreover, we attempted to investigate whether Model I could also be applied in the prediction of $CD4^+$ T cell responses which differ owing to the avidity of TCR-p:MHCII interactions. As previously stated, $CD4^+$ T cells responding to low avidity TCR ligation expand less and possess distinct subset compositions. Therefore, we modified the differentiation rates and proliferation rates of Model I in an attempt to model the low-avidity setting. These alterations to Model I enabled the computed model to accurately reflect the measured data that was produced from a population of $CD4^+$ T cells responding to low-avidity interactions (Fig. 23). Subsequently, we evaluated the fidelity of the Model I after adjusting proliferation parameters. Thus, we studied the proliferation capacity of $CD4^+$ T cells responding to high or low avidity TCR ligation by staining for bromodeoxyuridine (BrdU) incorporation. The proliferative activity was well described by the simulated Model I and further supported that the *in silico* data are in agreement with the biological attributes (Fig. 24). Taken together, the computational simulation is able to be applied to predict the fate decisions during T cell development and T cell responses influenced by novel

variables. Furthermore, our results indicate that single $CD4^+$ T cells outfitted with a TCR of defined avidity determine the average response emerging from multiple precursor T cells, yet individually present a probabilistic outcome.

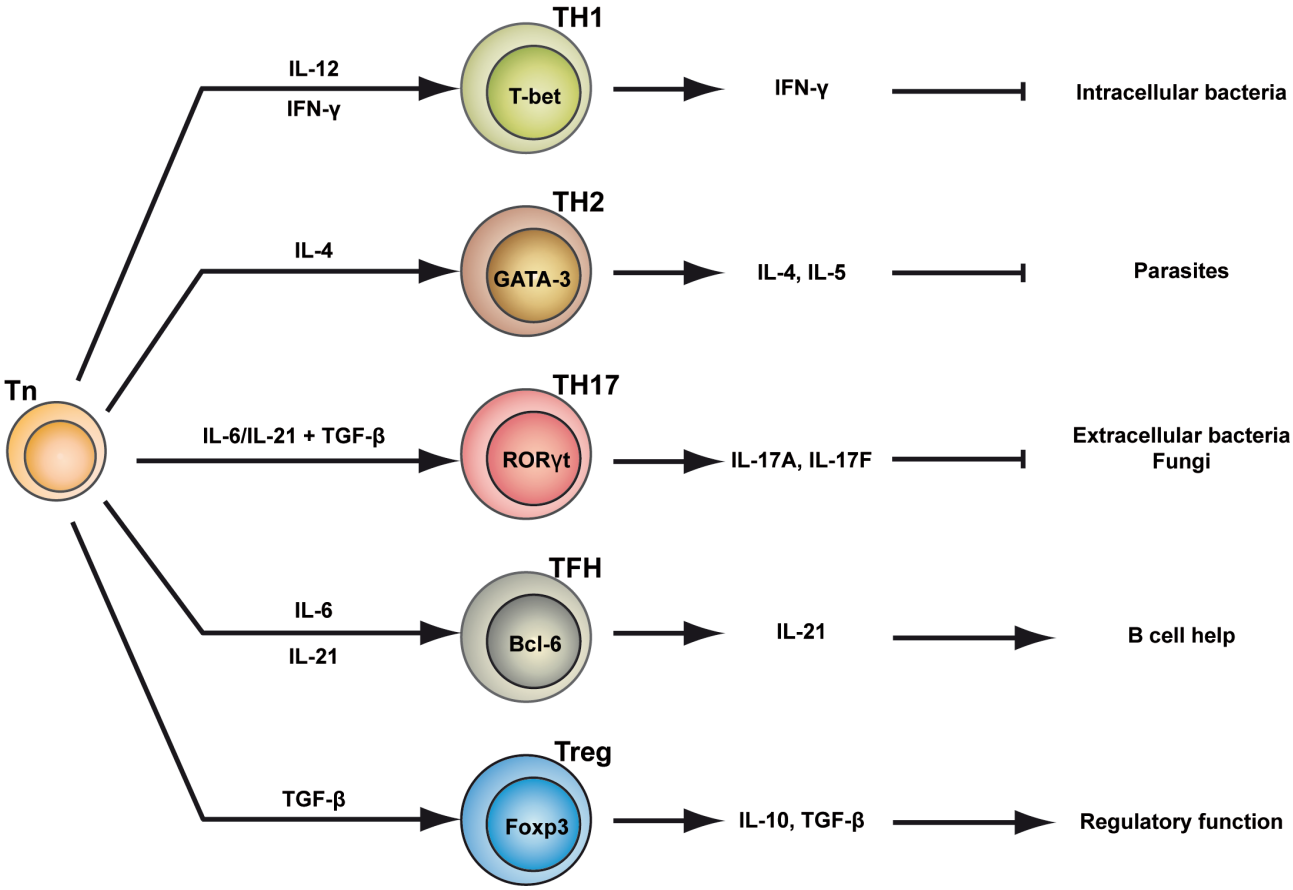

Fig 1. Polarization of naive CD4$^+$ T cells into distinct T helper cell subsets

These specific stimulatory cytokines influence signature transcription factor expression which directs naive CD4$^+$ T cells to TH1, TH2, TH17, TFH or Treg cell differentiation. Subsequently, the pattern of cytokine secretion characterizes the specific helper T cell subsets and their immune function. Abbreviations: IFN-γ, Interferon-γ; TGF-β, transforming growth factor-β; T-bet, T-box transcription factor; GATA3, GATA-binding factor 3; RORγt, retinoid-related orphan receptor-γt; Bcl-6, B-cell lymphoma 6; Foxp3, forkhead box protein 3; Tn, naive T cell; TH1, T helper 1 cell; TH2, T helper 2 cell; TH17, T helper 17 cell; TFH, follicular helper T cell; Treg, regulatory helper T cell.

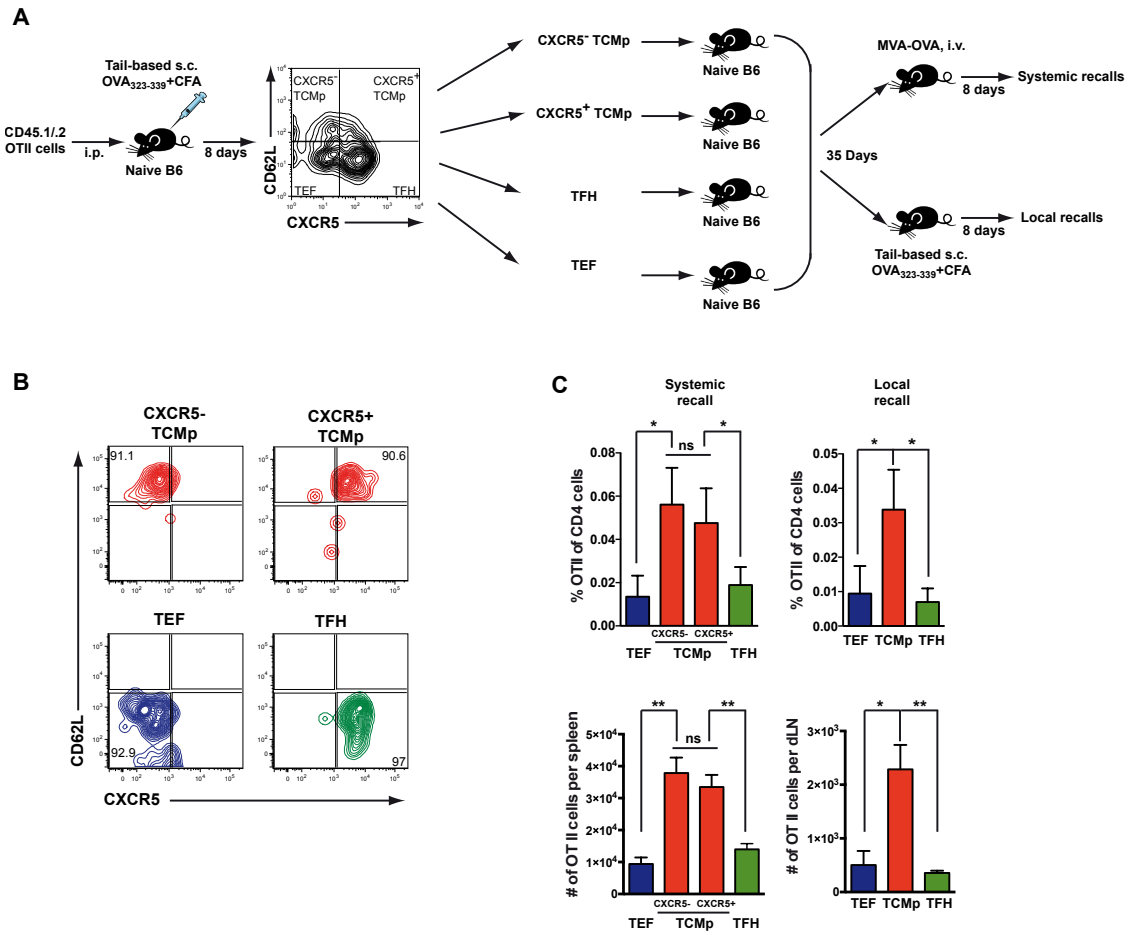

Fig 2. TCMp cells mount superior memory potential

(A-C) 10^4 naive $CD4^+CD25^-CD44^{lo}$ cells were sorted from the peripheral blood of OTII CD45.1 donor mice and adoptively transferred to C57BL/6 recipients, which were subcutaneously (s.c.) immunized at the tail base with $OVA_{323-339}$ (OVA_{WT}) peptide in Complete Freund's Adjuvant (CFA). Immune responses were monitored in draining lymph nodes (dLNs) at day 8 post-immunization (p.i.). **(A)** The experimental workflow displays the design for evaluating the memory potential of these CD4+ T cell subsets. **(B-C)** At day 8 p.i., antigen-experienced $CD4^+CD44^{hi}CD45.1^+$ T cells were sorted via flow cytometry into three or four subsets according to the expression of CXCR5 and CD62L, separately transferred into naïve secondary C57BL/6 recipients and 35 days later exposed to a systemic intravenous (i.v.) or local s.c. recall immunization with Modified Vaccinia Virus Ankara expressing OVA (MVA-OVA) or OVA_{WT} in CFA, respectively. **(B)** Contour plots indicate subset purity after flow-cytometric sorting. **(C)** Bar graphs show recall expansion derived from transferred subsets at day 8 after recall immunization (n=3-4). Error bars represent the SEM.

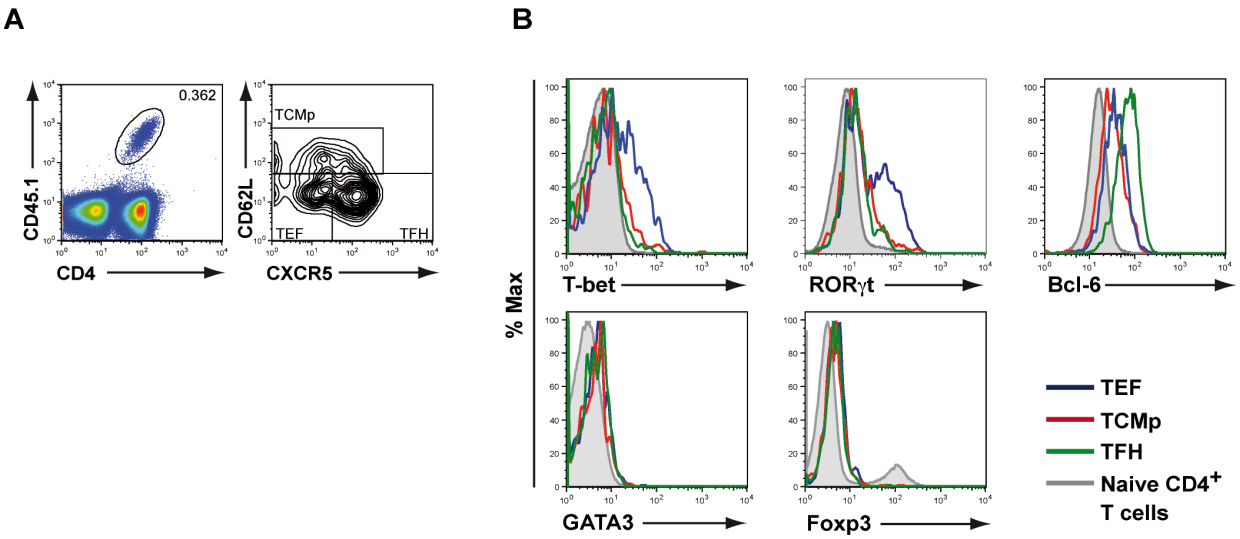

Fig 3. Three $OVA_{323-339}$-specific CD4+ T cell subsets are identified in draining lymph nodes

(A-B) 10^3-10^4 naive $CD4^+CD25^-CD44^{lo}$ cells were sorted from the peripheral blood of OTII CD45.1 donor mice and adoptively transferred to C57BL/6 recipients, which were subcutaneously (s.c.) immunized at the tail base with $OVA_{323-339}$ (OVA_{WT}) peptide in Complete Freund's Adjuvant (CFA). Immune responses were monitored in draining lymph nodes (dLNs) at day 8 post-immunization (p.i.). **(A)** Pseudo-color and contour plots show responding $CD4^+CD45.1^+$ T cells (number indicates percent of living leukocytes) and their phenotypic subdivision into $CXCR5^-CD62L^+$ TEF, $CD62L^+$ TCMp and $CXCR5^+CD62L^-$ TFH cells. **(B)** Histograms indicate the expression of lineage defining transcription factors T-bet, RORγt, Bcl-6, GATA3 and Foxp3 at day 8 p.i. in OTII T cells of TEF, TCMp and TFH phenotypes and in endogenous $CD4^+$ T cells of naïve phenotype.

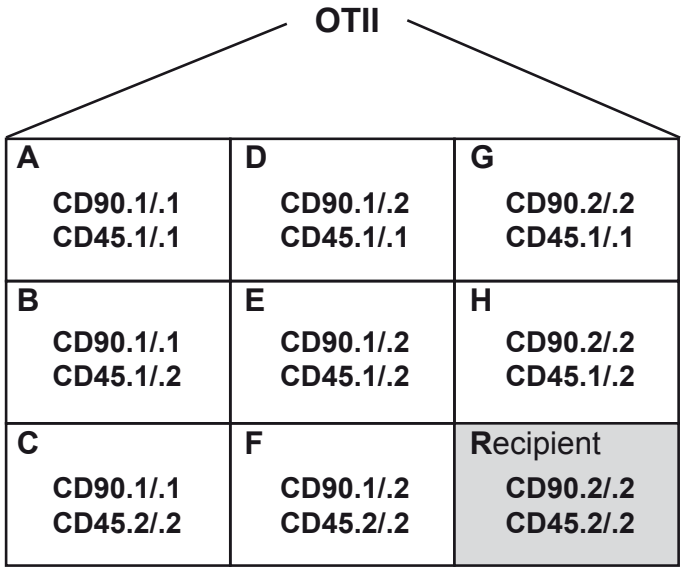

Fig 4. OTII congenic matrix mouse model

Scheme displays the congenic phenotypes from A to H and C57BL/6 recipient.

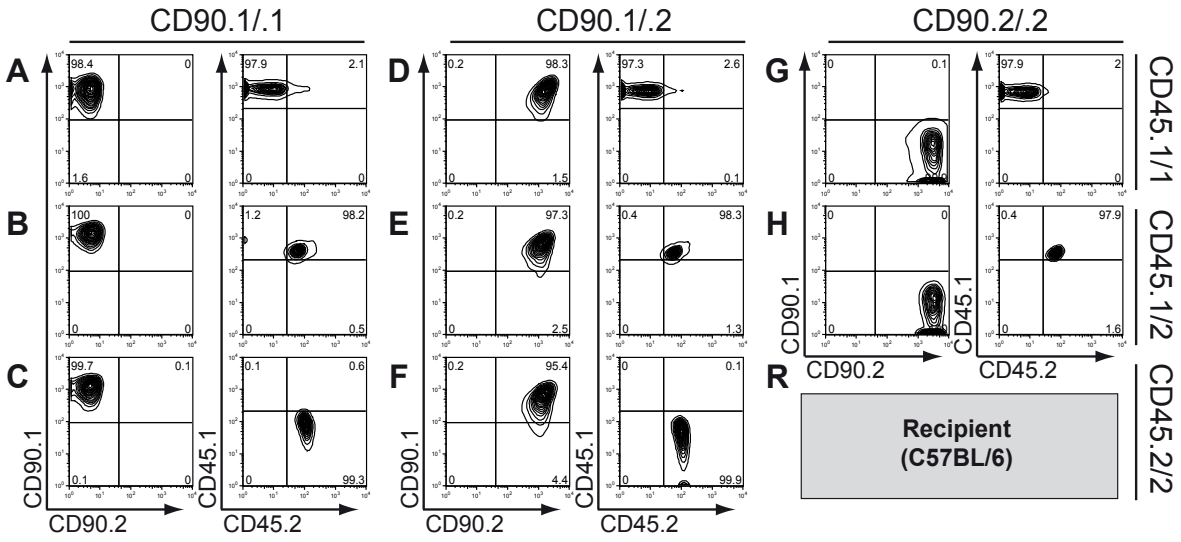

Fig 5. Identification of OTII congenic matrix cells

Flow-cytometric analysis of CD4+ T cells from the peripheral blood of OTII congenic donors for expression of CD45.1, CD45.2, CD90.1 and CD90.2. Recipient C57BL/6 mice are CD45.2/.2 and CD90.2/.2.

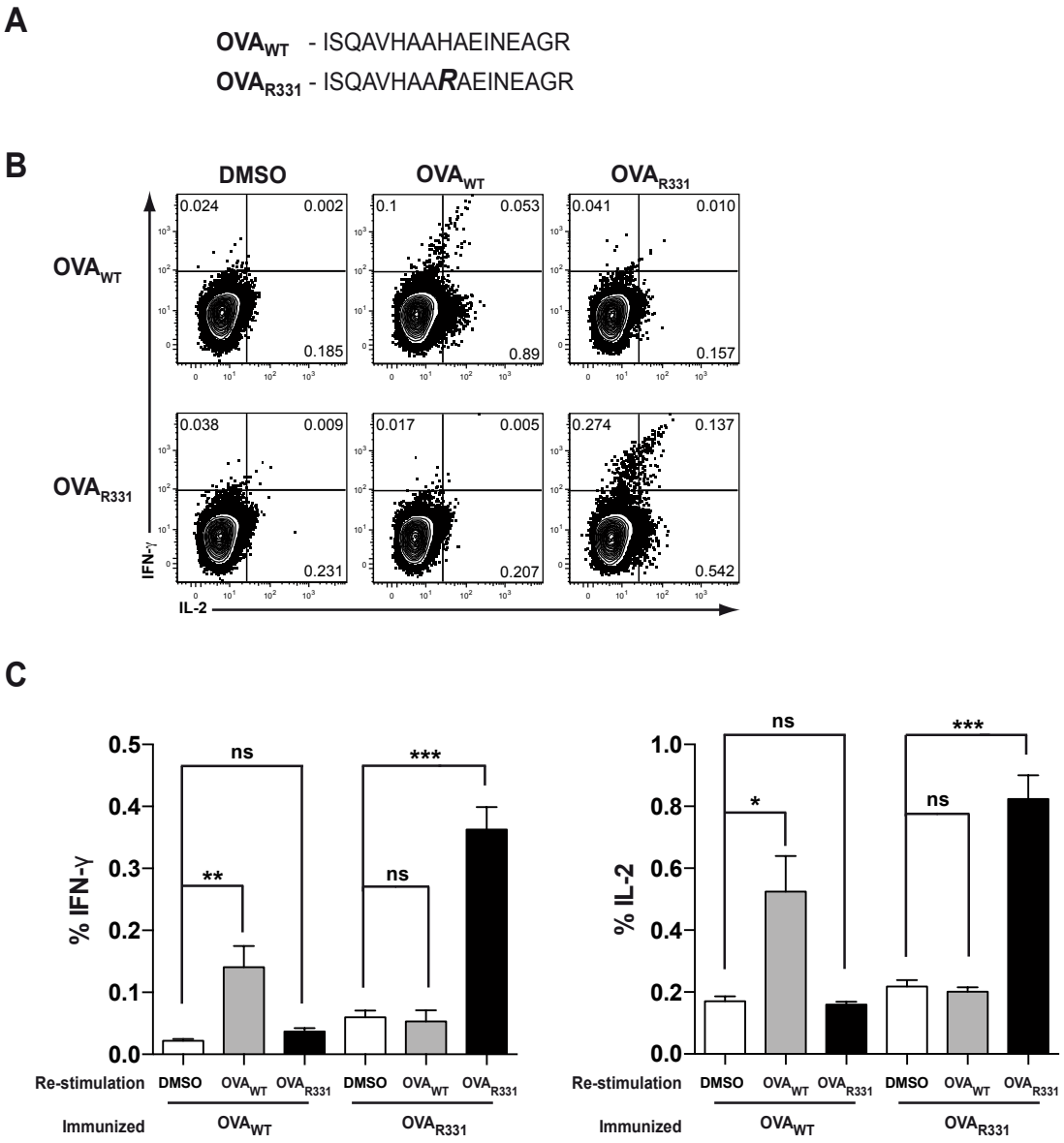

Fig 6. OVA$_{323-339}$ (OVA$_{WT}$) and Altered Peptide Ligand OVA$_{R331}$ induce peptide-specific responses derived from endogenous CD4$^+$ T cells

(A) Amino acid sequence of OVA$_{WT}$ and OVA$_{R331.}$ **(B-C)** C57BL/6 mice were subcutaneously (s.c.) immunized at the tail base with OVA$_{WT}$ or OVA$_{R331}$ in Complete Freund's Adjuvant (CFA). Immune responses were monitored in draining lymph nodes (dLNs) at day 8 post-immunization (p.i.). Cells derived from dLNs were re-stimulated in vitro with 1µg OVA$_{WT}$ or OVA$_{R331}$ both dissolved in dimethyl sulfoxide (DMSO) or cultures were supplemented with DMSO alone. **(B)** Dot plots are gated on CD4$^+$ T cells and show intracellular cytokine staining for interleukin-2 (IL-2) and interferon-γ (IFN-γ). Numbers indicate % of events per quadrant. **(C)** Bar graphs indicate mean percentage of IFN-γ and IL-2 positive cells among CD4$^+$ T cells in dLNs under distinct immunization and re-stimulation conditions (n=5).

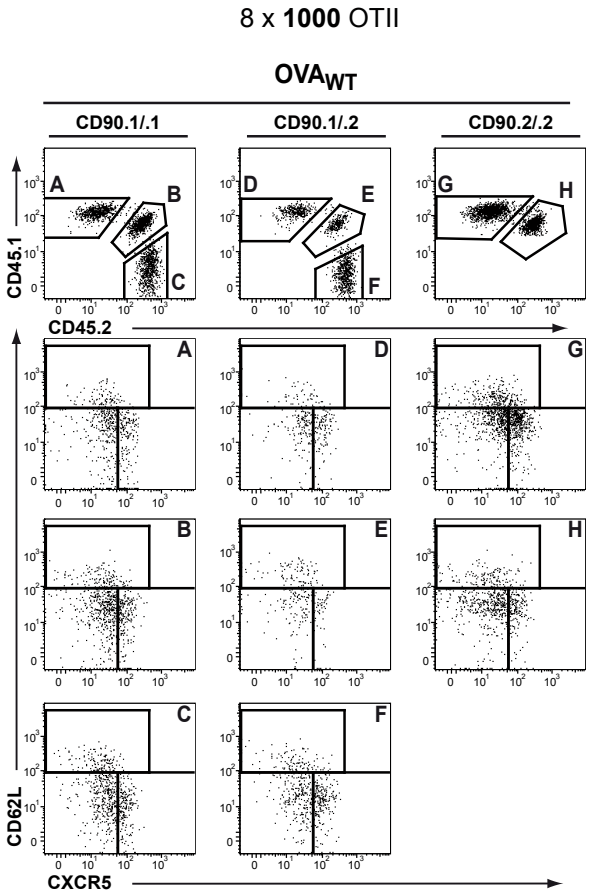

Fig 7. Progenies derived from 1000-OTII cells can be detected on day8 after OVA$_{323-339}$ peptide immunization

8x1000 CD4^{+}CD25^{-}CD44^{lo} cells were sorted via flow cytometry from eight OTII congenic donors expressing distinct combinations of the congenic markers CD45.1/.2 and CD90.1/.2 and transferred to C57BL/6 recipients followed by s.c. immunization with 100μg OVA$_{WT}$ peptide in CFA. Immune responses were monitored in dLNs at day 8 p.i. Dot plots show congenic phenotypes of recovered T cells (upper row) and the expression of CXCR5 and CD62L in congenic populations A-H (lower three rows).

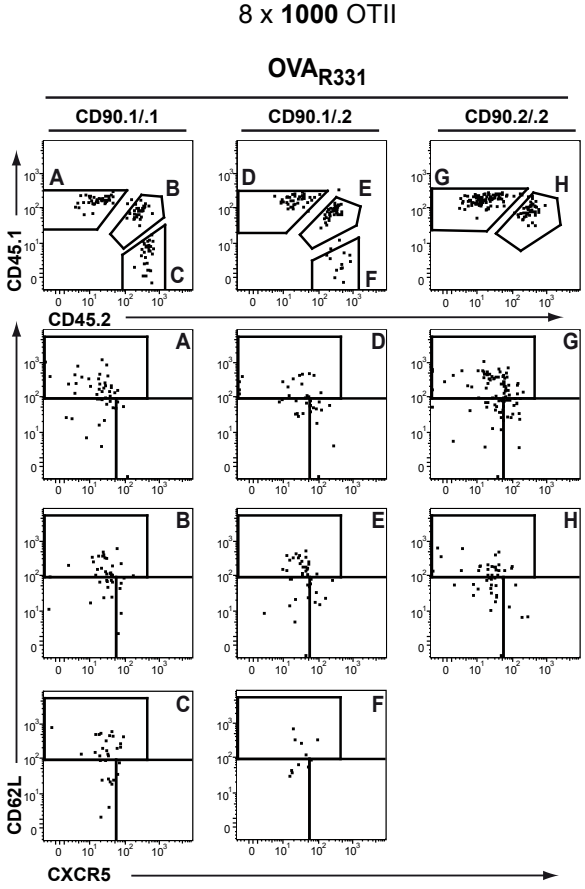

Fig 8. Progenies derived from 1000-OTII cells can be detected on day8 after OVA$_{R331}$ peptide immunization

8x1000 CD4^{+}CD25^{-}CD44^{lo} cells were sorted via flow cytometry from eight OTII congenic donors expressing distinct combinations of the congenic markers CD45.1/.2 and CD90.1/.2 and transferred to C57BL/6 recipients followed by s.c. immunization with 100μg OVA$_{R331}$ peptide in CFA. Immune responses were monitored in dLNs at day 8 p.i.. Exemplary dot plots show the congenic phenotypes of recovered T cells (upper row) and the expression of CXCR5 and CD62L in congenic populations A-H (lower three rows).

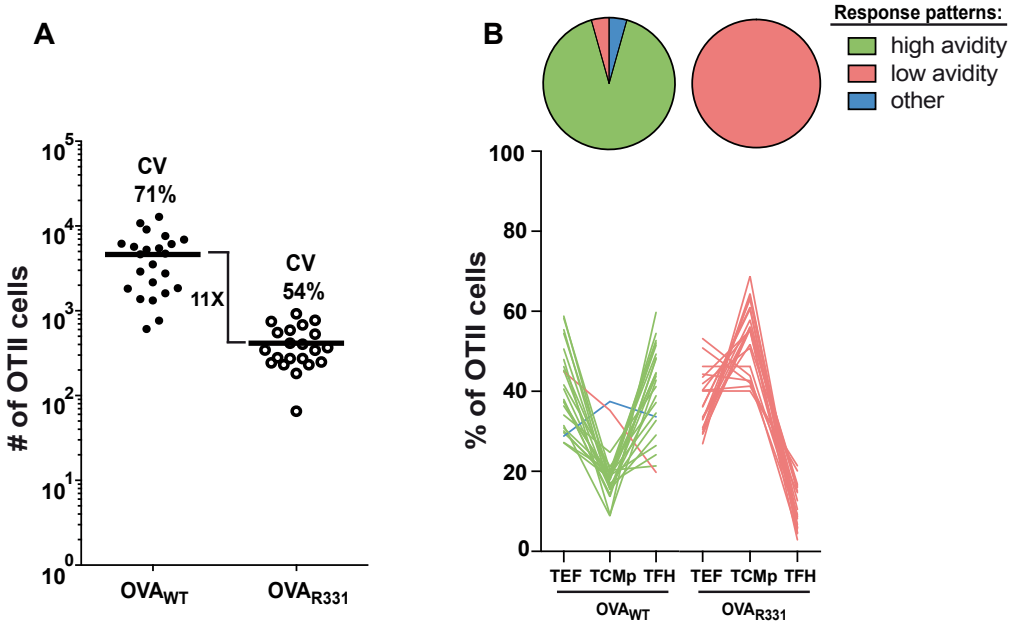

Fig 9. Avidity of TCR-p:MHCII interaction determines burst size and subset composition of population-derived responses

(A-B) 8x1000 CD4^{+}CD25^{-}CD44^{lo} cells were sorted via flow-cytometry from eight OTII congenic donors expressing distinct combinations of the congenic markers CD45.1/.2 and CD90.1/.2 and transferred to C57BL/6 recipients followed by s.c. immunization with 100μg of either OVA$_{WT}$ or OVA$_{R331}$ peptide in CFA. Immune responses were monitored in dLNs at day 8 p.i.. **(A)** Scatter plots indicate the absolute cell numbers recovered per transferred population A-H. Bar indicates mean. CV: coefficient of variation. **(B)** Line graphs indicate percentage of TEF, TCMp and TFH cells within each responding population. Each line stands for one response. Response patterns are defined as “high avidity” (green: TFH and TEF > TCMp), “low avidity” (red: TEF and TCMp > TFH) and “other” (blue: TFH and TCMp > TEF). Pie charts show relative prevalence of response patterns.

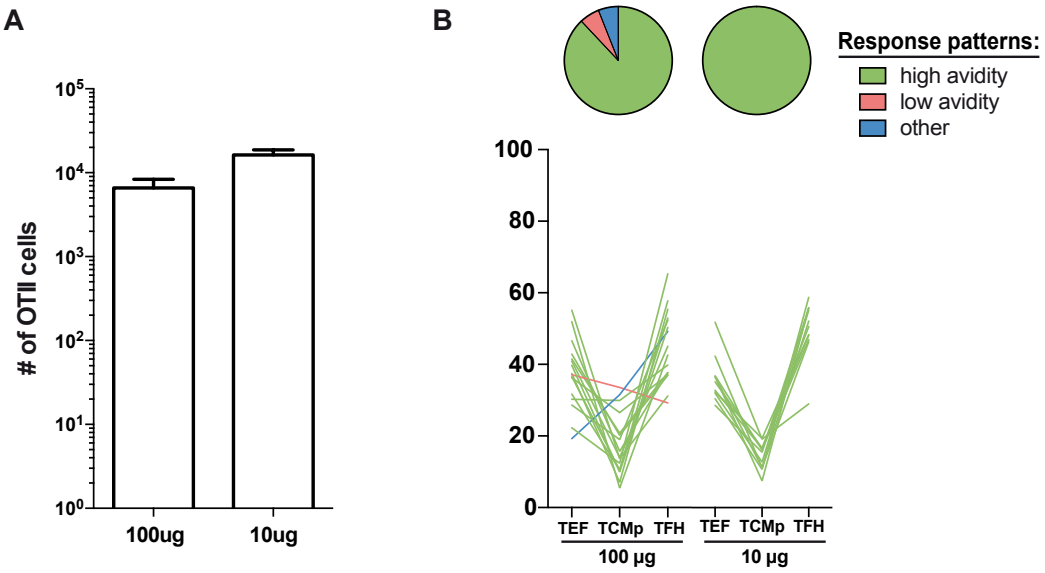

Fig 10. Ten-fold reduction in peptide dose does not substantially influence response patterns of OTII cell populations

(A-B) 1000 $CD4^{+}CD25^{-}CD44^{lo}$ cells were sorted via flow cytometry from OTII CD45.1 congenic donors and transferred to C57BL/6 recipients followed by s.c. immunization with either 100µg or 10µg OVA_{WT} in CFA. Immune responses were monitored in dLNs at day 8 p.i.. **(A)** Scatter plots indicate absolute cell number recovered per transferred population A-H. **(B)** Line plots indicate percentage of TEF, TCMp and TFH cells within each responding population. Each line stands for one response. Response patterns are defined as “high avidity” (green: TFH and TEF > TCMp), “low avidity” (red: TEF and TCMp > TFH) and “other” (blue: TFH and TCMp > TEF). Pie charts show relative prevalence of response patterns. Bars indicate mean, error bars indicate SEM.

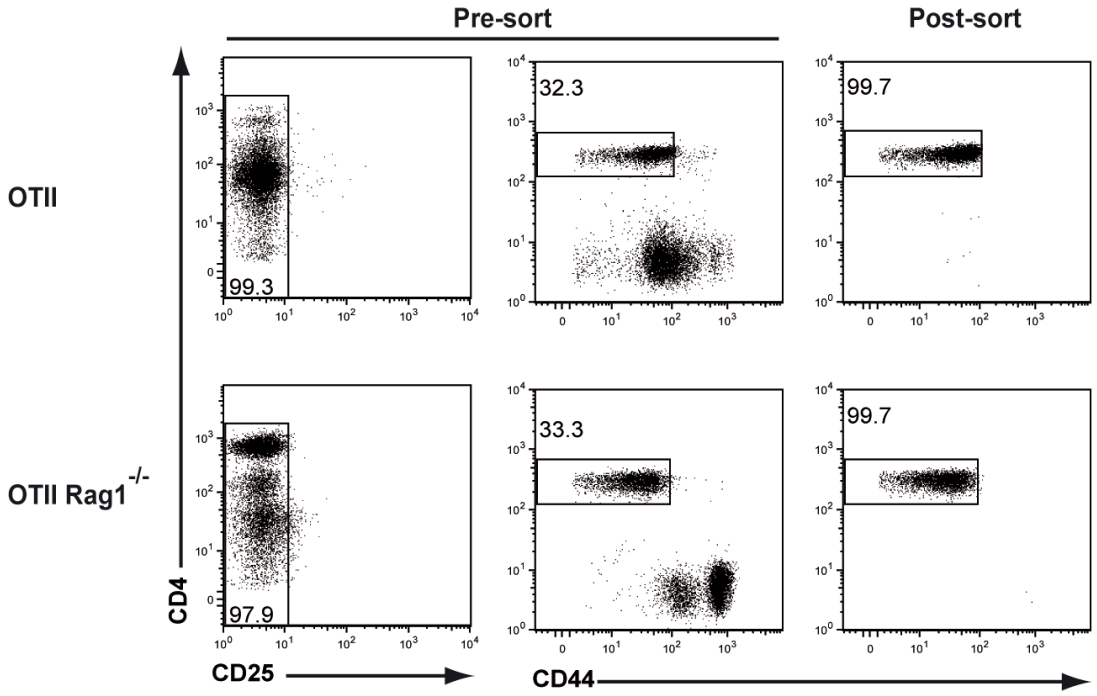

Fig 11. Flow cytometric sorting strategy and purity of sorted $CD4^{+}CD25^{-}CD44^{lo}$ cells harvested from peripheral blood of OTII and OTII $Rag1^{-/-}$ donors

Dot plots show gating strategy and sort purity for $CD4^{+}CD25^{-}CD44^{lo}$ cells sorted from peripheral blood of OTII and OTII $Rag1^{-/-}$ donors, respectively.

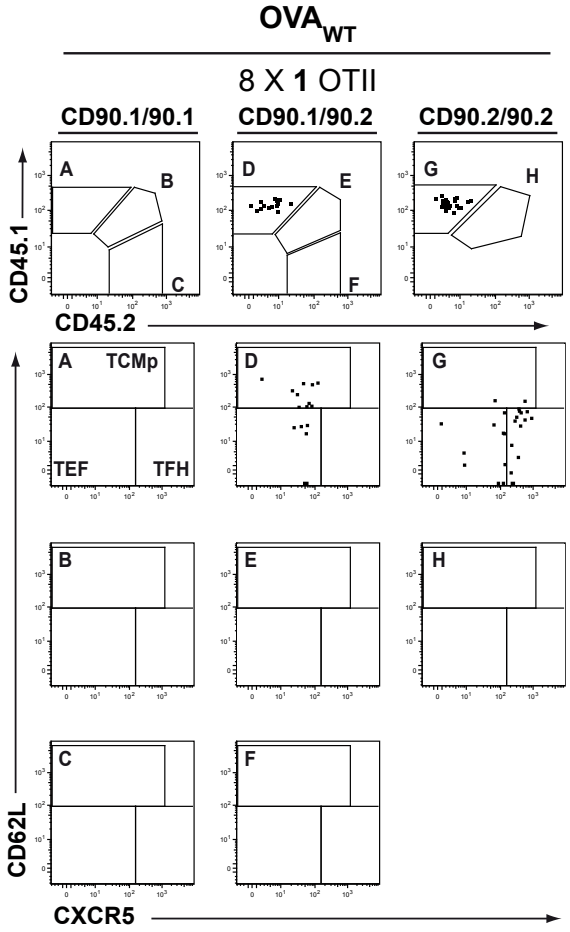

Fig 12. Peptide vaccination induces detectable progenies derived from a single CD4$^+$ T cell

8x1 CD4$^+$CD25$^-$CD44^{lo} cells were sorted via flow cytometry from eight OTII congenic donors and transferred to C57BL/6 recipients followed by s.c. immunization with 10μg of OVA$_{WT}$ peptide in CFA. Immune responses were monitored in dLNs at day 8 p.i.. Dot plots show congenic phenotype of recovered T cells (upper row) and expression of CXCR5 and CD62L in congenic populations A-H (lower three rows). Of note, two progenies recovered within the same recipient show distinct phenotypes.

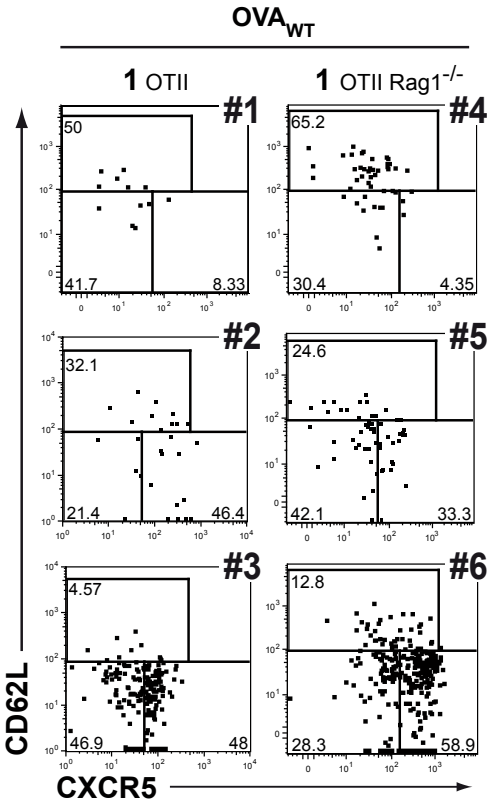

Fig 13. Phenotypic pattern of progenies derived from monoclonal single CD4$^+$ T cells exhibits high variability

8x1 CD4$^+$CD25$^-$CD44^{lo} cells were sorted via flow cytometry from eight OTII or OTII Rag1$^{-/-}$congenic donors and transferred to C57BL/6 recipients followed by s.c. immunization with 10μg of OVA$_{WT}$ peptide in CFA. Immune responses were monitored in dLNs at day 8 p.i.. Exemplary dot plots showing size and phenotype of progeny derived from single OTII (#1-3) or single OTII Rag1$^{-/-}$ cells (#4-6).

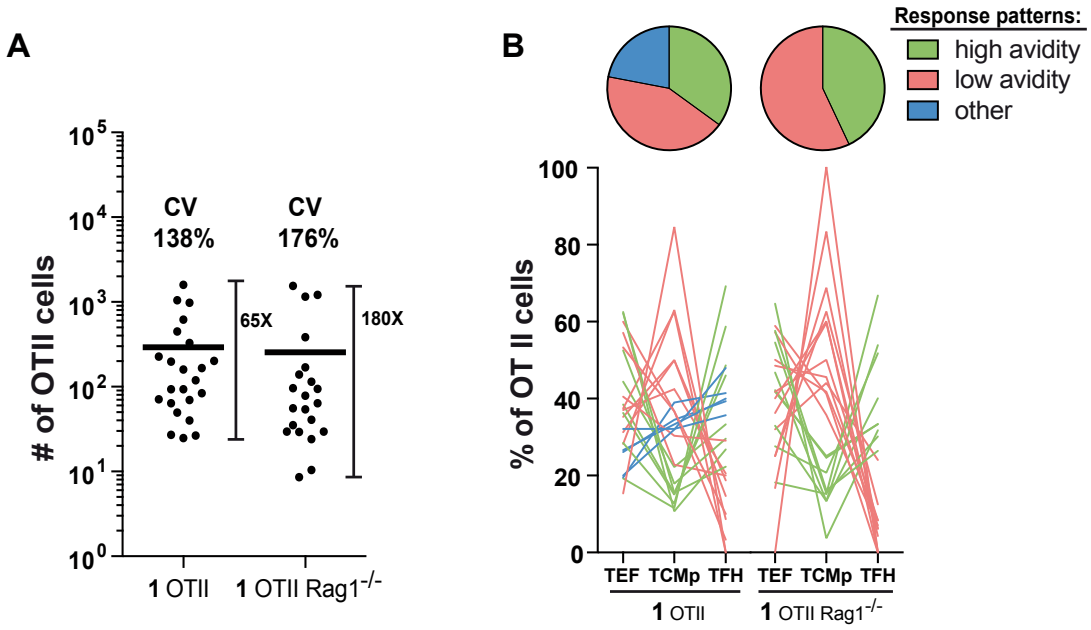

Fig 14. Single T cells respond stochastically to high avidity TCR ligation despite harboring identical TCRs

(A-B) 8x1 $CD4^+CD25^-CD44^{lo}$ cells were sorted via flow cytometry from eight OTII congenic or OTII $Rag1^{-/-}$ donors and transferred to C57BL/6 recipients followed by s.c. immunization with 10μg of OVA_{WT} peptide in CFA. Immune responses were monitored in dLNs at day 8 p.i.. **(A)** Scatter plots indicate absolute cell number recovered per transferred population A-H derived from single OTII or single OTII $Rag1^{-/-}$ cells. Bar indicates mean. CV: coefficient of variation. **(B)** Line graphs indicate percentage of TEF, TCMp and TFH cells within each responding population. Each line stands for one response. Response patterns are defined as “high avidity” (green: TFH and TEF > TCMp), “low avidity” (red: TEF and TCMp > TFH) and “other” (blue: TFH and TCMp > TEF). Pie charts show relative prevalence of response patterns.

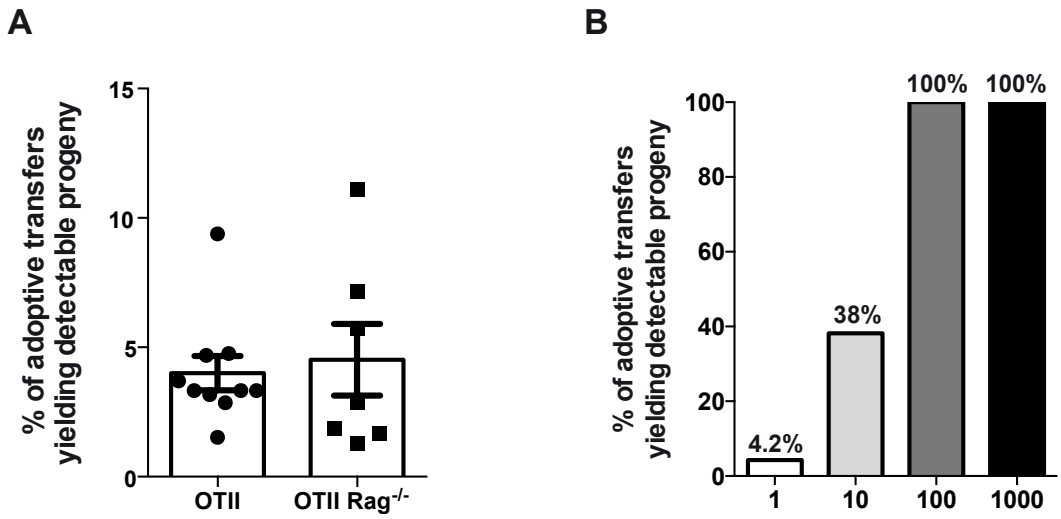

Fig 15. 4.2% take rate of single T cell transfer model

(A) Bars indicate the mean percentage of single T cell adoptive transfers in which progeny was detected. Full circles and full squares indicate % recovery in individual experiments utilizing OTII congenic or OTII Rag1$^{-/-}$ congenic donors, respectively. Error bars indicate SEM. **(B)** Bars indicate the mean percentage of 1-, 10-, 100- and 1000-OTII cell transfers that yielded detectable progeny. Of note, considering that 4.2% of single T cell transfers yielded detectable progeny, 10-, 100- and 1000-cell transfers are expected to yield detectable progeny in 34.9%, 98.6% and 100% of transfers, respectively. (n=44 for 1 cell, n=57 for 10 cells, n=51 for 100 cells and n=28 for 1000 cells).

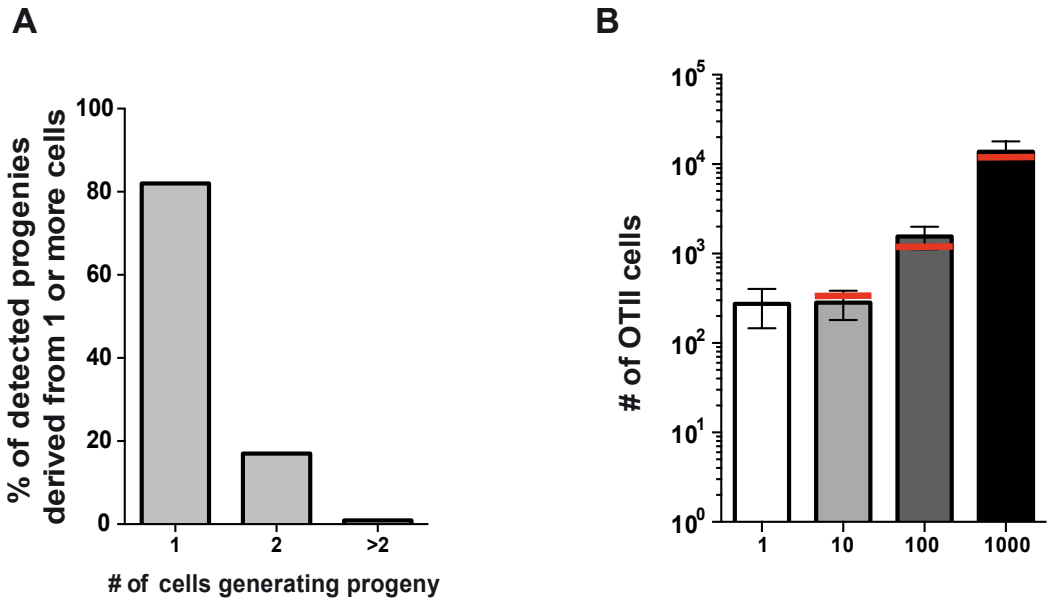

Fig 16. 10-cell transfers guarantee for more than 80% of recovered progenies to be derived from single OTII cells

(A) Bars indicate the expected percentage of progenies derived from 1, 2, or more than 2 cells after adoptive transfer of 10 naïve OTII cells. **(B)** Bars indicate the measured mean progeny size derived from 1, 10, 100 or 1000 adoptively transferred OTII cells. Error bars indicate the 95% confidence intervals. Red lines indicate the predicted mean progeny sizes that are expected when 4.2% of single T cell transfers yield detectable progeny. Predicted values for 10, 100 and 1000-cell transfers were generated by multiplying the mean size of single T cell-derived responses with 1.2, 4.2 and 42, respectively.

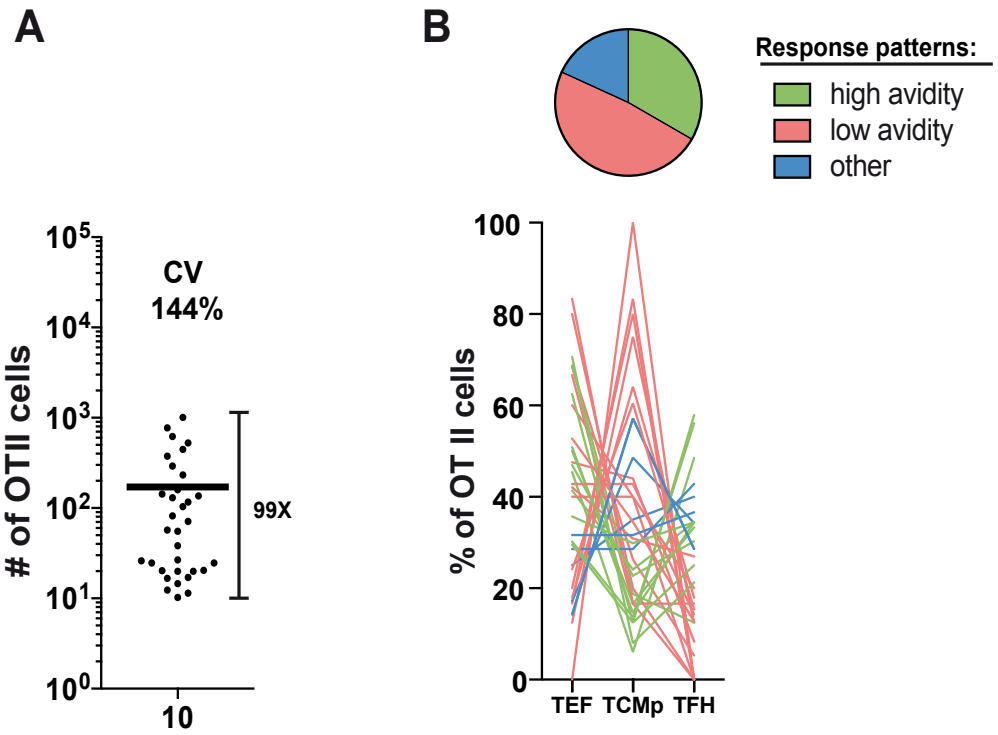

Fig 17. Very low cell number transfers confirm variation in T cell response size and phenotype

(A-B) 8x10 $CD4^+CD25^+CD44^{lo}$ cells were sorted via flow cytometry from eight OTII congenic donors and transferred to C57BL/6 recipients followed by s.c. immunization with 10μg of OVA_{WT} in CFA. Immune responses were monitored in dLNs at day 8 p.i.. **(A)** Absolute cell number detected after 10-cell transfers. Bar indicates mean. CV: coefficient of variation. **(B)** Percentage of TEF, TCMp and TFH cells within each progeny. Each line stands for one progeny. Response patterns are defined as "high avidity" (green: TFH and TEF > TCMp), "low avidity" (red: TEF and TCMp > TFH) and "other" (blue: TFH and TCMp > TEF). Pie charts show relative prevalence of response patterns.

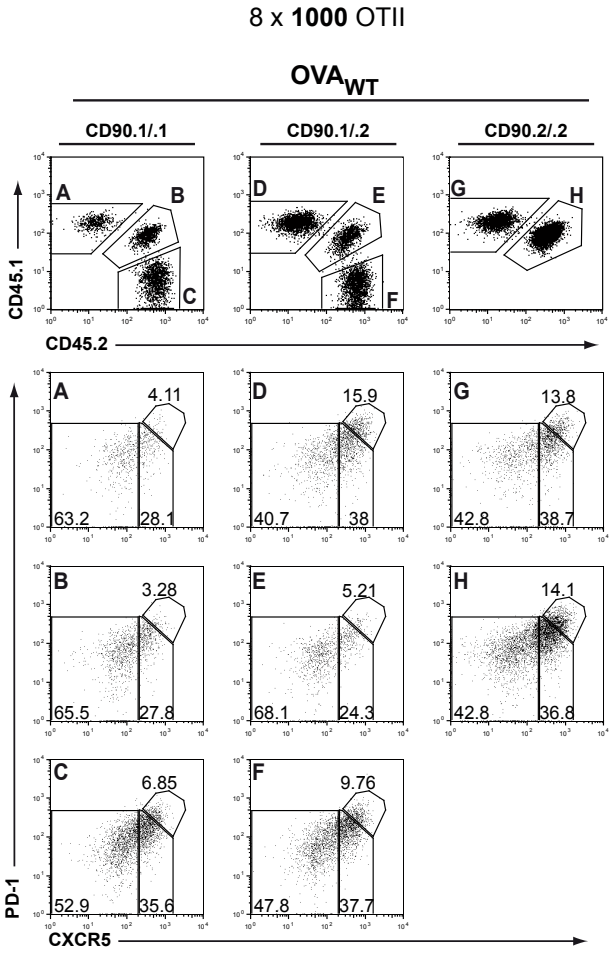

Fig 18. Analysis of cell subsets with CXCR5 and PD-1 discrimination on population level exhibits a consistent phenotypic pattern

8x1000 CD4^{+}CD25^{+}CD44^{lo} cells were sorted via flow cytometry from eight OTII congenic donors and transferred to C57BL/6 recipients followed by s.c. immunization with 10μg of OVA$_{WT}$ in CFA. Immune responses were monitored in dLNs at day 8 p.i.. Congenic phenotype of recovered T cells (upper row) and expression of CXCR5 and PD-1 in congenic populations A-H (lower three rows) after transferring 8x1000 cells are shown.

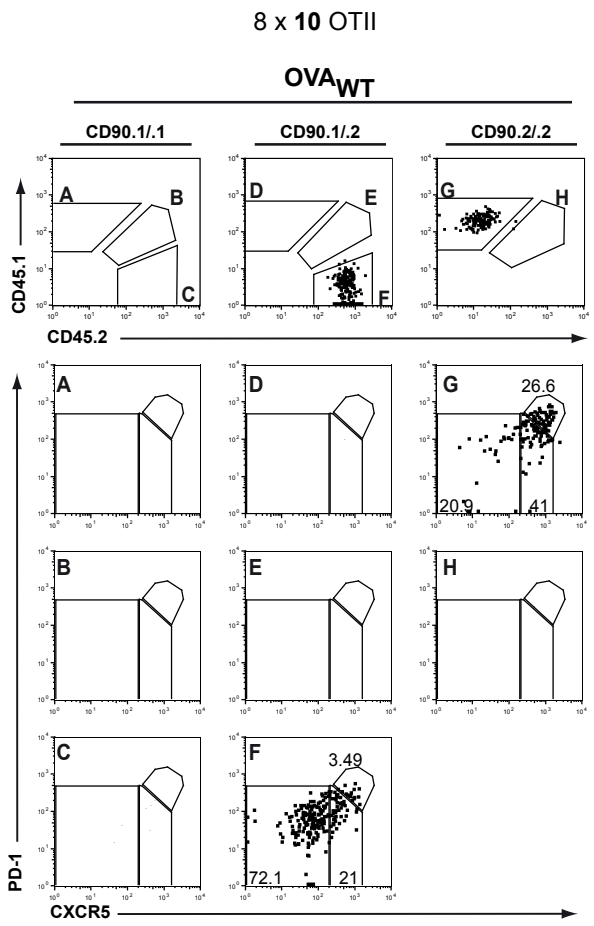

Fig 19. Distinct effector cell fate of progenies derived from 10-cell transfer via analysis of cell subsets with CXCR5 and PD-1 discrimination

8x10 $CD4^+CD25^+CD44^{lo}$ cells were sorted via flow cytometry from eight OTII congenic donors and transferred to C57BL/6 recipients followed by s.c. immunization with 10μg of OVA_{WT} in CFA. Immune responses were monitored in dLNs at day 8 p.i.. Congenic phenotypes of recovered T cells (upper row) and expression of CXCR5 and PD-1 in congenic populations A-H (lower three rows) after 8x10 cells are shown. Of note, progenies derived from 10 transferred T cells show distinct CXCR5/PD-1 phenotypes within the same recipient..

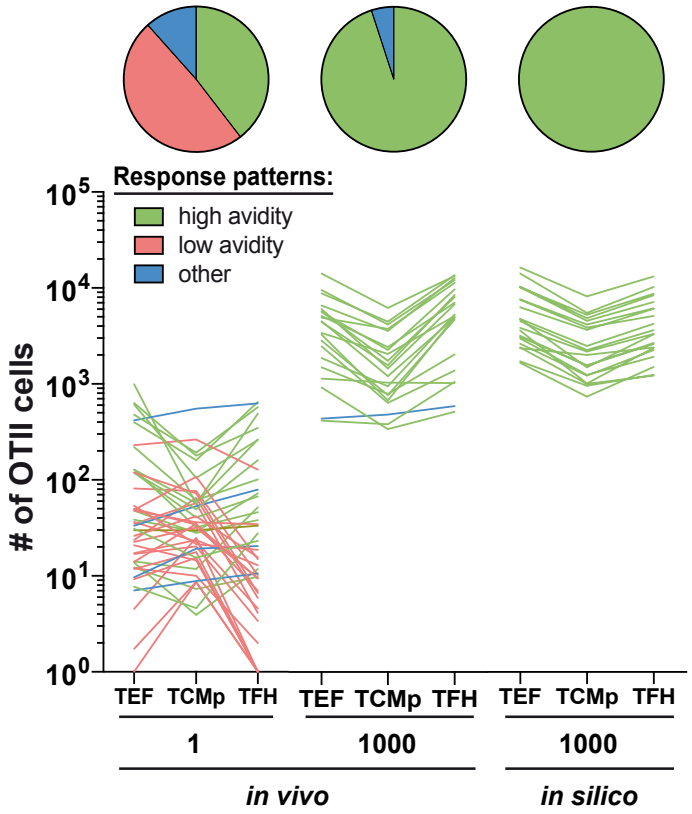

Fig 20. TCR avidity modulates the probability of stochastic division and differentiation events

Line plots indicate absolute numbers of TEF, TCMp and TFH cells recovered in dLNs after transfer of 1 or 1000 OTII cells and immunization with 10μg of OVA_{WT} plus CFA, or generated through in silico reconstruction of 1000-cell transfers by cumulating on average 42 randomly-drawn single T cell-derived responses.

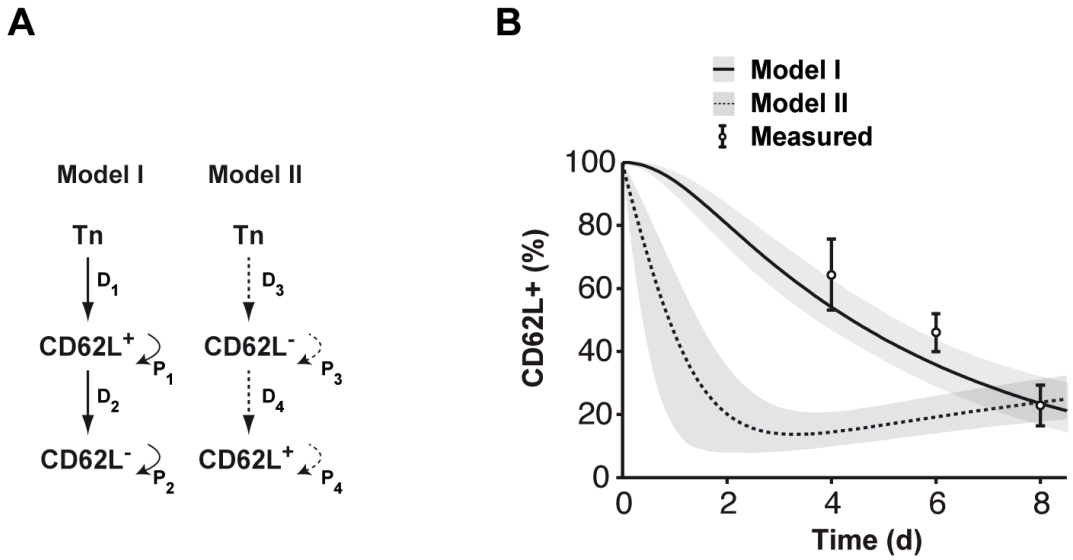

Fig 21. Stochastic Model I agree with measured CD4$^+$ T cell kinetic data

(A) Schematic depiction of two model structures in which CD62L$^-$ arise from CD62L$^+$ T cells (Model I: full lines) or vice versa (Model II: dashed lines). Differentiation and proliferation rates are indicated as D_1-D_4 and P_1-P_4. **(B)** Percentage of CD62L expressing cells during the first 8 days p.i. as predicted by the two models and as measured after transfer of OTII populations (circles with error bars indicate mean and STD; filled regions indicate 95% confidence prediction bands).

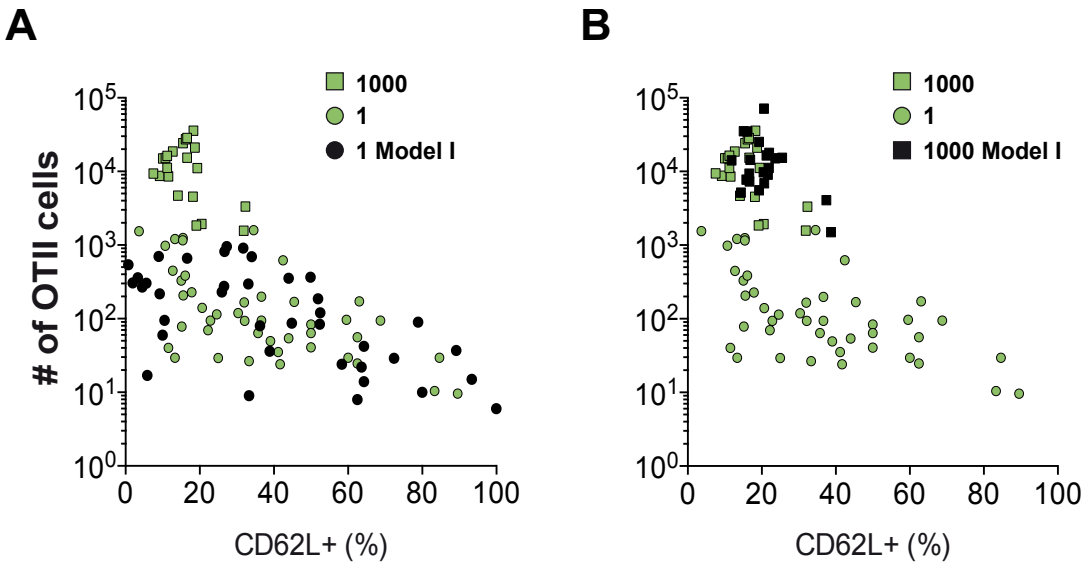

Fig 22. Stochastic Model I best fits CD4$^+$ T cell development under the condition of high TCR avidity ligation

(A-B) Scatter plots indicate the size (absolute cell number within dLNs) and phenotype (% CD62L positive cells) of progeny derived from single (green circles) or 1000 adoptively transferred T cells (green squares) after immunization with OVA_{WT} plus CFA or 1000 adoptively transferred T cells (red squares) after immunization with OVA_{R331} plus CFA. **(A)** Simulation of single T cell-derived progenies (black circles) using Model I. **(B)** Simulation of population-derived responses by cumulating an average of 42 simulations from (A) (black squares).

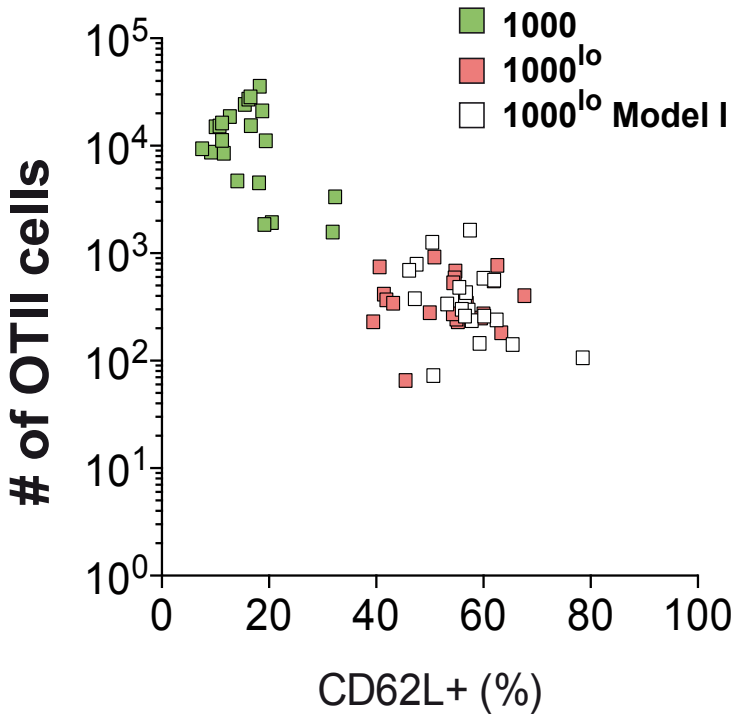

Fig 23. Stochastic Model I describes CD4$^+$ T cell respondse to low TCR avidity ligation

Scatter plots indicate the size (absolute cell number within dLNs) and phenotype (% CD62L positive cells) of progeny derived from single cell (green circles) or 1000 adoptively transferred T cells (green squares) after immunization with OVA_{WT} plus CFA or 1000 adoptively transferred T cells (red squares) after immunization with OVA_{R331} plus CFA. Simulations of population-derived responses by cumulating an average of 42 simulations from single T cell-derived progenies using Model I but with reduced proliferation and differentiation rates (white squares).

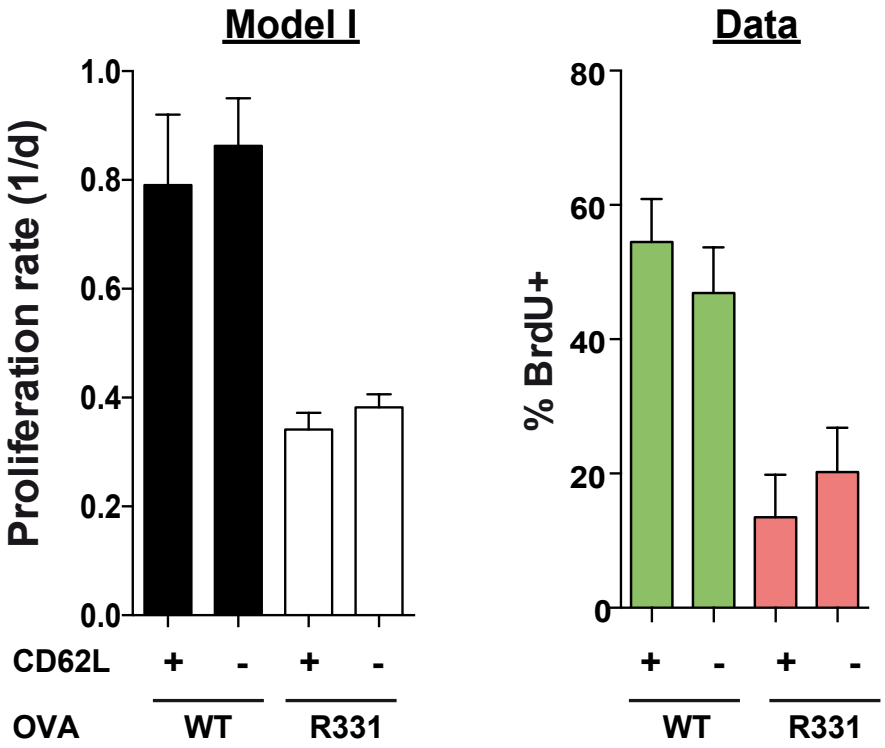

Fig 24. Proliferation rates of CD4$^+$ T cells responding to strong or weak binding peptides correlate to data predicted by Model I

Bar graphs show modeled mean proliferation rates or measured BrdU incorporation of CD62L$^+$ and CD62L$^-$ T cells at 6 days after high or low avidity TCR ligation with OVA_{WT} or OVA_{R331} in CFA. Error bars indicate SEM (data) and 95% confidence bounds (model I).

5. Discussion

5.1 Single cell analysis – the value of the congenic matrix model

Innovative single cell analysis techniques have advanced in the recent decade. The adoptive T cell transfer model has been applied as a powerful tool to dissect T cell development in a defined and rigorously controlled manner. It has been shown that the progenies derived from a SIINFEKL-specific single naïve $CD8^+$ T cell after infection with *Listeria monocytogenes* expressing OVA (L.m.-OVA) can be identified in the host at the peak response phase (82). Yet, in this laborious process, only one out of four mice having received a single naïve T cell will produce observable progeny. In the past, the T cell transfer model in combination with flow cytometry-based analysis was constrained due to the fact that transferred cells express a limited combination of congenic markers that can be used in an experimental setting to discriminate from host cells. Further improvement of the technique has overcome that obstacle and enabled the simultaneous tracking of up to eight single $CD8^+$ T cells in an identical immunological environment in the same recipient (84). This strategy greatly improves the efficiency of detecting immune responses derived form single $CD8^+$ T cells. Hence, the state-of-art 'congenic matrix model', which was established at the Institute of Microbiology, Immunology and Hygiene of the TUM, provides for an in-depth understanding of single cell fate decisions in vivo. Based on the success of this approach in monitoring $CD8^+$ T cell responses, a similar approach was developed for $CD4^+$ T cells. By multiplexed adoptive transfer of eight single OTII T cells, we were able to monitor single T cell-derived immune responses despite very low recovery rates of transferred T cells of less than 5%. A previous study showed that activated $CD4^+$ and $CD8^+$ T cells undergo distinct proliferative responses (94). $CD8^+$ T cells give rise to considerable clonal expansion, whereas $CD4^+$ T cells are subject to limited proliferation. Our study revealed that the detectable progenies derived from single $CD4^+$ T cells induced by a local immune response comprise approximately 4.2% of all transfers (Fig. 15). In comparison, the frequency of descendants generated from single $CD8^+$ T cells responding to a systemic infection ranges between 20 and 30%. In spite of these low recovery rates, the congenic matrix approach allowed for a sizeable number of single cell-derived immune responses to be monitored (Fig. 13-14).

5.2 Deterministic T cell receptor (TCR) avidity impacts the robust response

Naïve $CD4^+$ T cells bearing a variety of TCRs continually scan the antigen presenting cell (APC) network for cognate peptide:major histocompatibility class II (p:MHCII) complexes. The TCR-p:MHCII interaction is required for initiating naïve $CD4^+$ T cell expansion, as well as instructing subsequent effector T cell functions at later phases (62, 95). Published data support the concept that the avidity of TCR-p:MHCII interaction impacts the expansion and differentiation of $CD4^+$ T cells (67, 96).

In line with these observations, this thesis reveals that administration of the weak binding ligand R331, together with the depot-forming adjuvant (CFA), causes a reduction in the burst size of the population-derived response, when compared to the strong binding ligand $OVA_{323-339}$ (OVA_{WT}) (Fig. 9).

The published studies have indicated that diverse intensities of the TCR-p:MHCII interaction lead to biased generation of helper T cell subsets (79, 80). Specifically, a stronger TCR-p:MHCII ligation favors TFH cell polarization, while the commitment of the other effector helper T cell subsets selectively require weaker ligation. In this context, OVA_{WT} peptide immunization in vivo sufficiently elicits T Follicular Helper (TFH), T Central Memory precursor (TCMp) and T Effector Helper (TEF) cell compartments, which are defined by the effector functions and expression of the lineage-specific markers. In particular, the TEF cell compartment comprises two distinct effector Helper T cell subsets, which are T Helper 1 (TH1) and TH17 cells (Fig. 3). Due to the fact that TFH cells are a specialized subset supporting B cells producing high-avidity and long-term antibody production, the formation of this antigen-specific compartment requires a prolonged and high-avidity TCR-p:MHCII interaction for receiving adequate signals (35, 71). Hence, the $CD4^+$ T cells bearing TCRs with weakly binding p:MHCII interactions produce a considerable decrease in TFH cell compartments, whereas the strong binding interaction generates a large fraction of TEF and TFH cell subsets (Fig. 9). Previous research has revealed that p:MHCII density substantially modulates the polarization of Helper T cell subsets. However, our study suggests that a 10-fold drop in peptide density does not generate a drastic impact on the expansion and the composition of $CD4^+$ T cells (Fig. 10). Instead, an 11 times reduction of expansion size on T cells with low-avidity TCR ligation represents a clearly distinct burst size. Even though the distinct avidities influence the potency of T cell propagation, the robust response at the population level remains

consistent, which is independent of peptides generating either strong or weak TCR avidity ligation. Collectively, the population-derived progenies display an averaged response, whose differentiation pattern is tightly modulated by TCR avidity.

5.3 Probabilistic circumstances shape single CD4$^+$ T cell development

Naive CD4$^+$ T cell populations comprise diverse precursor cells specific to a wide spectrum of pathogenic peptides, the frequency of which varies from around 20 up to hundreds per mouse (97). Early studies analyzed p:MHCII-specific naïve CD4$^+$ T cell response on the population level, presenting an averaged response assembled from a polyclonal T cell population. Interestingly, each individual cell within the polyclonal repertoire composes a unique differentiation fate (88). However, our study, which also investigated single CD4$^+$ T cell responses emerging from a monoclonal repertoire, produced a stochastic response pattern derived under defined inflammatory conditions (Fig. 14). This conflict may arise due to the different cell subsets analyzed in these studies. Other groups using CXCR5 and PD-1 markers to discriminate TH1, TFH, and germinal center (GC)-TFH cells, restricted the detectable diversity of effector CD4$^+$ T cell phenotypes owing to the fact that TFH and GC-TFH cell subsets contain highly correlated genetic profiles (35). However, we used CXCR5 in combination with CD62L markers to identify TEF, TFH and TCMp cell subsets, and with that identified a hitherto unappreciated diversity of single CD4$^+$ T cell development. Additionally, we attempted to evaluate our observation by analyzing the phenotypes derived from a scant number of populations, a technique similar to a limiting dilution approach, with the application of the CXCR5 and PD-1 surface markers. Even though the diversity of effector cell types is indeed reduced when monitoring these markers, we were still able to identify distinct response patterns emerging after transfer of monoclonal 10-cell populations (Fig. 19). The results indicate that single T cells expressing identical TCRs generate a heterogeneous instead of homogenous cell fates, likely depending on the probabilistic events they encountered in the course of infection or vaccination.

Based on the tetramer-enrichment staining strategy, Listeriolysin O peptide (LLOp):I-A^b-specific CD4$^+$ T cell populations in a naïve polyclonal repertoire are estimated to comprise around 50 cells, and 2W:I-A^b-specific CD4$^+$ T cell populations are predicted to have around 160 cells (88). Nonetheless, epitope-specific naïve cell populations are competent in yielding a robust response of comparable size and phenotype of effector cells, despite

such a low frequency of precursor cells. This implies that a minimum of approximately 50 epitope-specific naïve T cells consisting of multiple clones is capable of inducing a robust immune response. In our study, the 4.2% of detectable progenies originating from single transferred $CD4^+$ T cells were incorporated into an *in silico* analysis to simulate the response pattern of a population of $CD4^+$ T cells. The data showed that assembly of 42 progenitor cells having identical TCR avidity could already restore the population response pattern, which is comparable to the expansion size and effector cell compositions generated from 1000 transferred T cells that is estimated to be a 42-cell derived-response on the basis of 4.2% recovery rate in this adoptive transfer system (Fig. 20). Therefore, this analysis suggested that the robustness of the response generated from an epitope-specific naïve $CD4^+$ T cell population harboring the same TCR requires the participation of at most 42 naïve precursors. In either case, a robust response is guaranteed when a sufficient number of p:MHCII-specific naïve $CD4^+$ T cells of identical or at least similar TCR avidity is present in the periphery. In summary, a population of $CD4^+$ T cells responding to cognate p:MHCII complexes will represent a unique response pattern, which reflects the cumulative responses of multiple precursor cells having experienced stochastic division and differentiation events.

Mathematical simulations from previous studies, which predicted a single $CD8^+$ T cell developmental hierarchy, are in accordance with a progressive differentiation model (84). In the present study we propose that the $CD62L^-$ effector cell subset originates from the $CD62L^+$ TCMp precursor cells and not vice versa. Computational analysis of responses derived from single $CD4^+$ T cells supported a model (Model I) that also presumed a developmental pathway of a $CD4^+$ T cells from naïve T cells to $CD62L^+$ TCMp cells and then to $CD62L^-$ T cell subsets. Model I best describes our in vivo observations regarding the behavior of populations of $CD4^+$ T cells responding to either high-avidity or low-avidity TCR-p:MHCII ligation. These simulation results suggest that $CD4^+$ T cell development may be also in line with progressive differentiation pathways proposed for $CD8^+$ T cells.

Remarkably, more than half of the single T cell-derived responses to high avidity TCR ligation displayed a differentiation pattern containing high fractions of TCMp cells, which resembles the “low avidity response pattern” identified on population level. This observation could be explained by the fact that, within a probabilistic environment, it is hard for a single cell to acquire a strong and stable signal that is the prerequisite for the production of $CD62L^-$ TFH and TEF cell subsets. This limited availability of high-quality signal is already sufficient to generate the TCMp cell population. It still remains to be elucidated how many precursor cells are sufficient to generate this small portion of

functional effector cells modulating the primary response, as well as the large fraction of memory cell populations which remain to mount an efficient response in a recall scenario. Interestingly, a previous study revealed that OT-I cells, infected by Listeria monocytogenes (Lm.) expressing cognate SIINFEKL peptide or Altered Peptide Ligands (APL) which induce low-avidity TCR ligation, were capable of inducing functional memory cells irrespective of the avidity of TCR ligation (98).

5.4 Stochastic influences contribute to the differentiation fate of $CD4^+$ T cell

TCR-p:MHCII interaction is the first stage of $CD4^+$ T cell development. Our research highlights the fact that the stochastic differentiation fate of single cells is fine-tuned by the deterministic influence of TCR avidity. However, intrinsic TCR avidity is only one of the factors influencing single cell fate decision. Transcription factors Blimp-1 and Bcl-6 are antagonistic molecules tightly regulating classic effector cell lineages and TFH cell diversification (34). The divergence of Blimp-1 and Bcl-6 expressing cells can be seen within 72 hours, which implies that Helper T cell subsets already commit at an early stage after T cell activation (99). A variety of cellular and soluble factors involved in the regulation of the initial event of $CD4^+$ T cell development have been intensively discussed. Besides the initial TCR signal, the second signal transmitted by costimulatory molecules must not be neglected. Antigen presenting cells including dendritic cells (DCs) and B cells express costimulatory molecules interacting with the receptors present on $CD4^+$ T cells. For example, the inducible costimulatory molecule (ICOS) plays an important role in controlling the development of naïve $CD4^+$ T cells into TFH cells. Deficiency of ICOS molecules has significant impacts on Bcl-6 induction that result in the loss of TFH production and B cell maturation (99). Additionally, this effect may cause up-regulation of Blimp-1 and CD25 (IL-2 receptor alpha chain, IL-2Rα) expression and prompt naïve T cells to differentiate into classical effector helper T cells. Of note, the expression of the surface marker CD25 is also induced early during T cell immune responses. The daughter cells which inherit the CD25 molecules receive an IL-2 signal, inducing a chain reaction which activates STAT5 and further induces Blimp-1 expressions (100). Therefore, the third signal given by the IL-2 cytokine is a crucial factor to balance the ratio of classic effector helper cells and TFH cells. It has been implied that the density of IL-2 cytokine in a secondary lymphoid organ is relatively high in the T cell zone where the classic effector helper T cells

are generated (101). In order to promote TFH cell polarization, $CD4^+$ T cells have to be recruited to the outer T cell zone, which makes contact with B cells, forming a specialized microenvironment. In that location, DCs produce membrane bound and soluble CD25 molecules to bind and dampen IL-2 cytokines, which causes down-regulation of Blimp-1 expression and facilitate the formation of TFH cells. Taken together, single naïve $CD4^+$ T cells re-circulate into secondary lymphoid organs and there encounter their cognate p:MHCII ligand. Hereafter, the fate decision of $CD4^+$ T cells is strongly influenced by the probabilistic circumstances such as the IL-2 cytokine density that influences the tendency of lineage-specific gene expression to control the production of effector cell types.

5.5 Clinical relevance

A well-functioning immune response requires quickly expanded effector cells to resolve the acute infection, as well as long-lasting memory cells to control any secondary infections that may arise. However, T cells gradually become dysfunctional in the setting of chronic infection or malignancy. As a result, adoptive T cell therapy has been developed to boost or restore the immune response when the immune system is impaired. As a compelling candidate, the $CD4^+$ T cell has been frequently exploited to support $CD8^+$ T cell persistence and also to help B cells in secreting large quantities of antibodies (102). Thus, how to provide a population of epitope-specific $CD4^+$ T cells with durable effector function has been intensively discussed. To achieve this clinically significant aim, the transferred $CD4^+$ T cells should be able to generate a population of efficient effector cells to accomplish instant control during the early infection phase. Meanwhile, they should also produce long-lived memory cells to enable meaningful secondary or chronic responses.

In vivo fate mapping of single T cells allows for better understanding the diversification of antigen-specific helper T cell subsets. With respect to the influence of TCR avidity, a population of $CD4^+$ T cells carrying high-avidity TCRs generates productive effector helper subsets but also TCMp cells, while those having low-avidity TCRs induce mainly TCMp cells. Concerning their developmental history, the incorporation of *in silico* analysis supported the perspective that the $CD62L^-$ classic effector cells originate from the $CD62L^+$ TCMp cell subset. For this reason, high-avidity TCR expressing T cells would effectively induce a large amount of acute effector cells to readily halt the infectious outbreak, while T cells harboring low-avidity TCRs produce mainly memory precursor cells potentially required during repeated pathogen encounters. Thus, the transfer of a mixture of naïve $CD4^+$ T cell populations harboring antigen-specific TCRs with high and low avidity might

facilitate the goal of simultaneously producing effective antigen-specific effector and memory T cells.

Taken together the data presented here show that key features of T cell immune responses to high avidity TCR ligation, such as the preferential generation of TFH cells (79), are not guaranteed by the clonal selection of an individual $CD4^+$ T cell expressing a high avidity TCR. Indirect evidence for such stochastic variation of T cell fate decisions has recently been gathered for human $CD4^+$ T cells (103). However, it has also been shown that most single $CD4^+$ T cells from a polyclonal TCR repertoire generate immunological memory in response to infection (89). In line with this observation we find that most single $CD4^+$ T cells indeed give rise to a sizeable number of TCMp cells (Fig. 20). Considering that T cell fate decisions are taken within a probabilistic framework, in which TCR avidity closely determines response outcomes only when multiple T cells are engaged, we propose that this primary expansion of a unique T cell clone into multiple TCMp cells is essential for allowing TCR avidity to reliably guide the course of secondary immune responses. These findings shed new light on the immunological principles underlying successful prime-boost vaccinations and have the potential to inform the optimal design of future immunotherapeutic approaches.

6. Summary

The interaction of the T cell receptor (TCR) and the peptide:major histocompatibility complex II (p:MHCII) initiates $CD4^+$ T cell proliferation and differentiation. The regulation of this response is influenced by TCR avidity, as shown by its strong impact on determining the size and phenotype of immune responses derived from populations of $CD4^+$ T cells. The role of TCR avidity in the differentiation of single $CD4^+$ T cells warrants further investigation.

In this thesis, adoptive transfer of single $CD4^+$ T cells or $CD4^+$ T cell populations, derived from OTII TCR-transgenic mice of distinct congenic phenotype, was applied in combination with subcutaneous immunization with $OVA_{323-339}$ (OVA_{WT}) peptide or the Altered Peptide Ligand OVA_{R331}. This vaccination strategy effectively induced three subsets: T Effector Helper cells (TEF), T Central Memory precursor cells (TCMp) and T Follicular Helper cells (TFH). These subsets were identified by surface marker staining and further characterized based on their transcription factor profiles and their capacity for secondary expansion during recall immune responses. We showed that immune responses derived from population of monoclonal $CD4^+$ T cells display a characteristic response pattern that is determined by the avidity of TCR ligation. However, single T cells carrying a TCR of defined avidity generate stochastic response patterns. Supported by computational analysis we show that TCR avidity does not determine the outcome of single T cell-derived immune responses but rather defines the likelihood with which single $CD4^+$ T cells take stochastic decision to divide or differentiate. These data argue that fate decisions of single $CD4^+$ T cells are taken within a probabilistic frame work, in which TCR avidity closely determines response outcomes only when multiple T cells expressing the same TCRs – or TCRs of similar avidity – are engaged.

7. List of references

1. Zell T., Khoruts A., Ingulli E., Bonnevier J. L., Mueller D. L., Jenkins M. K. Single-cell analysis of signal transduction in CD4 T cells stimulated by antigen in vivo. PNAS. 2001;98:10805-10.

2. Schwartz R.H. T cell anergy. Annu Rev Immunol. 2003;21:305-34.

3. Hogquist K. A., Tolinson A. J. , Kieper W. C., McGargill M. A., Hart M. C., Naylor S., et al. Identification of a naturally occuring ligand for thymic positive selection. Immunity. 1997;6:389-99.

4. Zal T., Volkmann A., Stockinger B. Mechanisms of tolerance induction in major histocompatibility complex class II-restricted T cells specific for a blood-borne self-antigen. J Exp Med. 1994;180:2089-99.

5. Coffman R. L., Seymour B. W. P., Lebman D. A., Hiraki D. D., Christiansen J. A., Shrader B., et al. The role of helper T cell products in mouse B cell differentiation and isotype regulation. Immunological Reviews. 1988;102:5-28.

6. Galli S. J., Tsai M. Mast cells in allergy and infection: versatile effector and regulatory cells in innate and adaptive immunity. Eur J Immunol. 2010;40(7):1843-51.

7. Ye P., Rodriguez F. H., Kanaly S., Stocking K. L., Schurr J., Schwarzenberger P., et al. Requirement of interleukin 17 receptor signaling for lung CXC chemokine and granulocyte colony-stimulating factor expression, neutrophil recruitment, and host defense. J Exp Med. 2001;194:519-27.

8. Kumar P., Chen K., Kolls J.K. Th17 cell based vaccines in mucosal immunity. Curr Opin Immunol. 2013;25(3):373-80.

9. Ansel K. M., McHeyzer-Williams L. J., Ngo V. N., McHeyzer-Williams M. G., Cyster J. G. In vivo-activated CD4 T cells upregulate CXC chemokine receptor 5 and reprogram their response to lymphoid chemokines. J Exp Med. 1999;190:1123-34.

10. Breitfeld D., Ohl L., Kremmer E., Ellwart J., Sallusto F., Lipp M., et al. Follicular B helper T cells express CXC chemokine receptor 5, localize to B cell follicles, and support immunoglobulin production. J Exp Med. 2000;192:1545-51.

11. Schaerli P., Willimann K., Lang A. B., Lipp M., Loetscher P., Moser B. CXC Chemokine receptor 5 expression defines follicular homing T cells with B cell helper function. J Exp Med. 2000;192:1553-62.

12. Kim C. H., Rott L. S., Clark-Lewis I., Campbell D. J., Wu L., Butcher E. C. Subspecialization of CXCR5+ T cells: B helper activity is focused in a germinal center-localized subset of CXCR5+ T cells. J Exp Med. 2001;193:1373-81.

13. Reinhardt R. L., Liang H. E., Locksley R. M. Cytokine-secreting follicular T cells shape the antibody repertoire. Nat Immunol. 2009;10(4):385-93.

14. Corthay A. How do regulatory T cells work? Scand J Immunol. 2009;70(4):326-36.

15. Josefowicz S. Z., Lu L. F., Rudensky A. Y. Regulatory T cells: mechanisms of differentiation and function. Annu Rev Immunol. 2012;30:531-64.

16. Mosmann V. R., Cherwinski H., Bond M. W., Giedlin M. A., Coffman R. L. Two Types Of Murine Helper T Cell Clone. The Journal of Immunology. 1986;136(7):2348-57.

17. Szabo S. J., Kim S. T., Costa G. L., Zhang X., Fathman C. G., Glimcher L. H. A novel transcription factor, T-bet, directs the Th1 lineage commitment. Cell. 2000;100:655-69.

18. Ouyang W., Loehning M., Gao Z., Assenmacher M., Ranganath S., Radbruch A., et al. Stat6-independent GATA-3 autoactivation directs IL-4-independent Th2 development and commitment. Immunity. 2000;12:27-37.

19. Sakaguchi S., Sakaguchi N., Asano M., Itoh M., Toda M. Immunologic self-tolerance maintained by activated T cells expressing IL-2 receptor a-chain (CD25). Breakdow of a single mechanism of self-tolerance causes various autoimmune diseases. J Immunol. 1995;186:3808-21.

20. Fontenot J. D., Gavin M. A., Rudensky A. Y. Foxp3 programs the development and function of CD4+CD25+ regulatory T cells. Nat Immunol. 2003;4(4):330-6.

21. Williams L. M., Rudensky A. Y. Maintenance of the Foxp3-dependent developmental program in mature regulatory T cells requires continued expression of Foxp3. Nat Immunol. 2007;8(3):277-84.

22. Hori S., Nomura T., Sakaguchi S. Control of regulatory T cell development by the transcription factor Foxp3. Science. 2003;299(5609):1057-61.

23. Brooks D. G., Walsh K. B., Elsaesser H., Oldstone M. B. IL-10 directly suppresses CD4 but not CD8 T cell effector and memory responses following acute viral infection. Proc Natl Acad Sci U S A. 2010;107(7):3018-23.

24. Beser O. F., Conde C. D., Serwas N. K., Cokugras F. C., Kutlu T., Boztug K., et al. Clinical features of interleukin 10 receptor gene mutations in children with very early-onset inflammatory bowel disease. J Pediatr Gastroenterol Nutr. 2015;60(3):332-8.

25. Schmidt A., Oberle N., Krammer P. H. Molecular mechanisms of treg-mediated T cell suppression. Front Immunol. 2012;3:51.

26. Brunkow M. E., Jeffery E. W., Hjerrild K. A., Paeper B., Clark L. B., Yasayko S., et al. Disruption of a new forkhead/winged-helix protein, scurfin, results in the fatal lymphoproliferative disorder of the scurfy mouse. Nat Gen 2001;27:68-73.

27. Bennett C. L., Christie J., Ramsdell F., Brunkow M. E., Ferguson P. J., Whitesell L., et al. The immune dysregulation, polyendocrinopathy, enteropathy, X-linked syndrome (IPEX) is caused by mutations of FOXP3. Nat Gen. 2001;27:20-1.

28. Harrington L. E., Hatton R. D., Mangan P. R., Turner H., Murphy T. L., Murphy K. M., et al. Interleukin 17-producing CD4+ effector T cells develop via a lineage distinct from the T helper type 1 and 2 lineages. Nat Immunol. 2005;6(11):1123-32.

29. Park H., Li Z., Yang X. O., Chang S. H., Nurieva R., Wang Y. H., et al. A distinct lineage of CD4 T cells regulates tissue inflammation by producing interleukin 17. Nat Immunol. 2005;6(11):1133-41.

30. Peck A., Mellins E. D. Precarious balance: Th17 cells in host defense. Infect Immun. 2010;78(1):32-8.

31. Ivanov, I. I., McKenzie B. S., Zhou L., Tadokoro C. E., Lepelley A., Lafaille J. J., et al. The orphan nuclear receptor RORgammat directs the differentiation program of proinflammatory IL-17+ T helper cells. Cell. 2006;126(6):1121-33.

32. Korn T., Bettelli E., Oukka M., Kuchroo V. K. IL-17 and Th17 Cells. Annu Rev Immunol. 2009;27:485-517.

33. Miossec P., Korn T., Kuchroo V. K. Interleukin-17 and type 17 helper T cells. The New England Journal of Medicine. 2009;361:888-98.

34. Johnston R. J., Poholek A. C., DiToro D., Yusuf I., Eto D., Barnett B., et al. Bcl6 and Blimp-1 are reciprocal and antagonistic regulators of T follicular helper cell differentiation. Science. 2009;325(5943):1006-10.

35. Crotty S. Follicular helper CD4 T cells (TFH). Annual review of immunology. 2011;29:621-63.

36. Ma C. S., Deenick E. K., Batten M., Tangye S. G. The origins, function, and regulation of T follicular helper cells. The Journal of experimental medicine. 2012;209(7):1241-53.

37. Swain S. L., Weinberg A. D., English M., Huston G. IL-4 directs the development of Th2-like helper effectors. The Journal of Immunology. 1990;145:3796-806.

38. Gros G. L., Ben-Sasson S. Z., Seder R., Finkelman F. D., Paul W. generation of interleukin 4 (IL-4)-producing cells in vivo and in vitro: IL-2 and IL-4 are required for in vitro generation of IL-4-producing cells. J Exp Med. 1990;172:921-9.

39. Hsieh C., Macatonia S. E., Tripp C. S., Wolf S. F., O' Garra A., Murphy K. M. Development of TH1 CD4+ T cells through IL-12 produced by Listeria-induced macrophages. Science. 1993;260:547-9.

40. Lighvani A. A., Frucht D. M., Jankovic D., Yamane H., Aliberti J., Hissong B. D., et al. T-bet is rapidly induced by interferon-g in lymphoid and myeloid cells. PNAS. 2001;98:15137-42.

41. Chen W., Jin W., Hardegen N., Lei K., Li L., Marinos N., et al. Conversion of peripheral CD4+CD25- naive T cells to CD4+CD25+ regulatory T cells by TGF-b induction of transcription factor Foxp3. J Exp Med. 2003;198:1875-86.

42. Davidson T. S., DiPaolo R. J., Andersson J., Shevach E. M. Cutting Edge: IL-2 Is Essential for TGF- -Mediated Induction of Foxp3+ T Regulatory Cells. The Journal of Immunology. 2007;178(7):4022-6.

43. Bettelli E., Carrier Y., Gao W., Korn T., Strom T. B., Oukka M, et al. Reciprocal developmental pathways for the generation of pathogenic effector TH17 and regulatory T cells. Nature. 2006;441(7090):235-8.

44. Mangan P. R., Harrington L. E., O'Quinn D. B., Helms W. S., Bullard D. C., Elson C. O., et al. Transforming growth factor-beta induces development of the T(H)17 lineage. Nature. 2006;441(7090):231-4.

45. Korn T., Bettelli E., Gao W., Awasthi A., Jager A., Strom T. B., et al. IL-21 initiates an alternative pathway to induce proinflammatory T(H)17 cells. Nature. 2007;448(7152):484-7.

46. Nurieva R. I., Chung Y., Hwang D., Yang X. O., Kang H. S., Ma L., et al. Generation of T follicular helper cells is mediated by interleukin-21 but independent of T helper 1, 2, or 17 cell lineages. Immunity. 2008;29(1):138-49.

47. Vogelzang A., McGuire H. M., Yu D., Sprent J., Mackay C. R., King C. A fundamental role for interleukin-21 in the generation of T follicular helper cells. Immunity. 2008;29(1):127-37.

48. Afkarian M., Sedy J. R., Yang J., Jacobson N. G., Cereb N., Yang S. Y., et al. T-bet is a STAT1-induced regulator of IL-12R expression in naive CD4+ T cells. Nat Immunol. 2002;3(6):549-57.

49. Thierfelder W. E., van Deursen J. M., Yamamoto K., Tripp R. A., Sarawar S. R., Carson R. T., et al. Requirement for Stat4 in interleukin-12-mediated response of natural killer and T cells. Nature. 1996;382:171-4.

50. Kaplan M. H., Sun Y., Hoey T., Grusby M. J. Impaired IL-12 responses and enhanced development of Th2 cells in Stat4-deficient mice. Nature. 1996;382:174-7.

51. Takada K., Tanaka T., Shi W., Matsumoto M., Minami M., Kashiwamura S-I., et al. Essential role of Stat6 in IL-4 signaling. Nature. 1996;380:627-30.

52. Shimoda K., van Deursen J., Sangster M. Y., Sarawar S. R., Carson R. T., Tripp R. A., et al. Lack of IL-4-induced Th2 response and IgE class switching in mice with disrupted Stat6 gene. Nature. 1996;380:630-3.

53. Laurence A., Tato C. M., Davidson T. S., Kanno Y., Chen Z., Yao Z., et al. Interleukin-2 signaling via STAT5 constrains T helper 17 cell generation. Immunity. 2007;26(3):371-81.

54. Burchill M. A., Yang J., Vogtenhuber C., Blazar B. R., Farrar M. A. IL-2 Receptor -Dependent STAT5 Activation Is Required for the Development of Foxp3+ Regulatory T Cells. The Journal of Immunology. 2006;178(1):280-90.

55. Yao Z., Kanno Y., Kerenyi M., Stephens G., Durant L., Watford W. T., et al. Nonredundant roles for Stat5a/b in directly regulating Foxp3. Blood. 2007;109:4368-75.

56. Ho I-C., Hodge M. R., Rooney J. W., Glimcher L. H. The proto-oncogene c-maf is responsible for tissue-specific expression of interleukin-4. Cell. 1996;85:973-83.

57. Ho I-C., Lo D., Glimcher L. H. c-maf promotes T helper cell type 2 (Th2) and attenuates Th1 differentiation by both interleukin 4-dependent and -independent mechanisms. J Exp Med. 1998;188:1859-66.

58. Lazarevic V., Chen X., Shim J. H., Hwang E. S., Jang E., Bolm A. N., et al. T-bet represses T(H)17 differentiation by preventing Runx1-mediated activation of the gene encoding RORgammat. Nat Immunol. 2011;12(1):96-104.

59. Djuretic I. M., Levanon D., Negreanu V., Groner Y., Rao A., Ansel K. M. Transcription factors T-bet and Runx3 cooperate to activate Ifng and silence Il4 in T helper type 1 cells. Nat Immunol. 2007;8(2):145-53.

60. Lohoff M., Mak T. W. Roles of interferon-regulatory factors in T-helper-cell differentiation. Nat Rev Immunol. 2005;5(2):125-35.

61. Jelley-Gibbs D. M., Lepak N. M., Yen M., Swain S. L. Two distinct stages in the transition from naive CD4 T cells to effectors, early antigen-dependent and late cytokine-driven expansion and differentiation. Journal of immunology (Baltimore, Md : 1950). 2000;165(9):5017-26.

62. van Panhuys N. TCR signal strength alters T-DC activation and interaction times and directs the outcome of differentiation. Front Immunol. 2016;7:1-14.

63. Hosken N. A., Shibuya K., Heath A. W., Murphy K. M., O' Garra A. The effect of antigen dose on CD4 T helper cell phenotype development in a T cell receptor-ab-transgenic model. J Exp Med. 1995;182:1579-84.

64. Constant S., Pfeiffer C., Woodard A., Pasqualini T., Bottomly K. Extent of T cell receptor ligation can determine the functional differentiation of naive CD4 T cells. J Exp Med. 1995;182.

65. Leitenberg D., Boutin Y., Constant S., Bottomly K. CD4 regulation of TCR signaling and T cell differentiation following stimulation with peptides of different affinities for the TCR. J Immunol 1998;161:1194-203.

66. Tubo N. J., Jenkins M. K. TCR signal quantity and quality in CD4+ T cell differentiation. Trends in Immunology. 2014:1-6.

67. van Panhuys N., Klauschen F., Germain R. N. T-cell-receptor-dependent signal intensiy dominantly controls CD4+ T cell polarization in vivo. Immunity. 2014;41:63-74.

68. Miller M. J., Wei S. H., Cahalan M. D., Parker I. Autonomous T cell trafficking examined in vivo with intravital two-photon microscopy. PNAS. 2003;100:1604-9.

69. Bajenoff M., Egen J. G., Koo L. Y., Laugier J. P., Brau F., Glaichenhaus N., et al. Stromal cell networks regulate lymphocyte entry, migration, and territoriality in lymph nodes. Immunity. 2006;25(6):989-1001.

70. Shiner E. K., Holbrook B. C., Alexander-Miller M. A. CD4+ T cell subset differentiation and avidity setpoint are dictated by the interplay of cytokine and antigen mediated signals. PLoS One. 2014;9(6):e100175.

71. Vinuesa C. G., Cyster J. G. How T cells earn the follicular rite of passage. Immunity. 2011;35(5):671-80.

72. Baumjohann D., Preite S., Reboldi A., Ronchi F., Ansel K. M., Lanzavecchia A., et al. Persistent antigen and germinal center B cells sustain T follicular helper cell responses and phenotype. Immunity. 2013;38(3):596-605.

73. Turner M. S., Kane L. P., Morel P. A. Dominant role of antigen dose in CD4+Foxp3+ regulatory T cell induction and expansion. J Immunol. 2009;183(8):4895-903.

74. George T. C., Bilsborough J., Viney J. L., Norment A. M. High antigen dose and activated dendritic cells enable Th cells to escape regulatory T cell-mediated suppression in vitro. Eur J Immunol. 2003;33:502-11.

75. Long S. A., Rieck M., Tatum M., Bollyky P. L., Wu R. P., Muller I., et al. Low-dose antigen promotes induction of FOXP3 in human CD4+ T cells. J Immunol. 2011;187(7):3511-20.

76. Kim C., Williams M. A. Nature and nurture: T-cell receptor-dependent and T-cell receptor-independent differentiation cues in the selection of the memory T-cell pool. Immunology. 2010;131(3):310-7.

77. Pfeiffer C., Stein J., Southwood S., Ketelaar H., Sette A., Bottomly K. Altered peptide ligands can control CD4 T lymphocyte differentiation in vivo. J Exp Med. 1995;181:1569-74.

78. Savage P., Boniface J. J., Davis M. M. A kinetic basis for T cell receptor repertoire selection during an immune response. Immunity. 1999;10(4):485-92.

79. Fazilleau N., McHeyzer-Williams L. J., Rosen H., McHeyzer-Williams M. G. The function of follicular helper T cells is regulated by the strength of T cell antigen receptor binding. Nature immunology. 2009;10(4):375-84.

80. Milner J. D., Fazilleau N., McHeyzer-Williams M., Paul W. Cutting edge: lack of high affinity competition for peptide in polyclonal CD4+ responses unmasks IL-4 production. J Immunol. 2010;184(12):6569-73.

81. Gottschalk R., Corse E., Allison J. P. TCR ligand density and affinity determine peripheral induction of Foxp3 in vivo. The Journal of experimental medicine. 2010;207(8):1701-11.

82. Stemberger C., Huster K. M., Koffler M., Anderl F., Schiemann M., Wagner H., et al. Disparate individual fates compose robust CD8 T cell immunity. Immunity. 2007;27(6):985-97.

83. Gerlach C., van Heijst J. W., Swart E., Sie D., Armstrong N., Kerkhoven R. M., et al. One naive T cell, multiple fates in CD8+ T cell differentiation. J Exp Med. 2010;207(6):1235-46.

84. Buchholz V. R., Flossdorf M., Hensel I., Kretschmer L., Weissbrich B., Gräf P., et al. Disparate individual fates compose robust CD8+ T cell immunity. Science (New York, NY). 2013;340(6132):630-5.

85. Gerlach C., Rohr J. C., Perié L., van Rooij N., van Heijst J. W. J, Velds A., et al. Heterogeneous differentiation patterns of individual CD8+ T cells. Science (New York, NY). 2013;340(6132):635-9.

86. Graef P., Buchholz V. R., Stemberger C., Flossdorf M., Henkel L., Schiemann M., et al. Serial transfer of single-cell-derived immunocompetence reveals stemness of CD8+ central memory T cells. Immunity. 2014;41:116-26.

87. Schepers K., Swart E., van Heijst J. W. J., Gerlach C., Castrucci M., Sie D., et al. Dissecting T cell lineage relationships by cellular barcoding. The Journal of experimental medicine. 2008;205(10):2309-18.

88. Tubo N. J., Pagán A. J., Taylor J. J., Nelson R. W., Linehan J. L., Ertelt J. M., et al. Single naive CD4+ T cells from a diverse repertoire produce different effector cell types during infection. Cell. 2013;153(4):785-96.

89. Tubo N. J., Fife B. T., Pagán A. J., Kotov D. I., Goldberg M. F., Jenkins M. K. Most microbe-specific naive CD4+ T cells produce memory cells during infection. Science. 2016;351:511-4.

90. Blattman J. N., Antia R., Sourdive D. J. D., Wang X., Kaech S. M., Murali-Krishna K., et al. Estimating the precursor frequency of naive antigen-specific CD8 T cells. J Exp Med. 2002;195:657-64.

91. Buchholz V. R., Schumacher T. N., Busch D. H. T Cell Fate at the Single-Cell Level. Annu Rev Immunol. 2016;34:65-92.

92. Constant S., Pfeiffer C., Woodard A., Pasqualini T., Bottomly K. Extent of T cell receptor ligation can determine the functional differentiation of naive CD4 T cells. J Exp Med. 1995;182:1591-6.

93. Robertson J. M., Jensen P. E., Evavold B. D. DO11.10 and OT-II T cells recognize a C-terminal ovalbumin 323-339 epitope. Journal of immunology (Baltimore, Md : 1950). 2000;164:4706-12.

94. Foulds K. E., Zenewicz L., Shedlock D. J., Jiang J., Troy A. E., Shen H. Cutting edge: CD4 and CD8 T cells are intrinsically different in their proliferative responses. Journal of immunology (Baltimore, Md : 1950). 2002;168(4):1528-32.

95. Obst R., van Santen H-M., Mathis D., Benoist C. Antigen persistence is required throughout the expansion phase of a CD4+ T cell response. J Exp Med. 2005;201:1555-65.

96. Fahmy T. M., Bieler J. G., Edidin M., Schneck J. Increased TCR avidity after T cell activation: a mechanism for sensing low-density antigen. Immunity. 2001;14:135-43.

97. Moon J. J., Chu H. H., Pepper M., McSorley S. J., Jameson S. C., Kedl R. M., et al. Naive CD4(+) T cell frequency varies for different epitopes and predicts repertoire diversity and response magnitude. Immunity. 2007;27(2):203-13.

98. Zehn D., Lee S. Y., Bevan M. J. Complete but curtailed T-cell response to very low-affinity antigen. Nature. 2009;458(7235):211-4.

99. Choi Y. S., Kageyama R., Eto D., Escobar T. C., Johnston R. J., Monicelli L., et al. ICOS receptor instructs T follicular helper cell versus effector cell differentiation via induction of the transcriptional repressor Bcl6. Immunity. 2011;34:932-46.

100. Martins G., Calame K. Regulation and functions of Blimp-1 in T and B lymphocytes. Annu Rev Immunol. 2008;26:133-69.

101. Li J., Lu E., Yi T., Cyster J. G. EBI2 augments Tfh cell fate by promoting interaction with IL-2-quenching dendritic cells. nature. 2016;533:110-4.

102. Aubert R. D., Kamphorst A. O., Sarkar S., Vezys V., Ha S-J., Barber D. L., et al. Antigen-specific CD4 T-cell help rescues exhausted CD8 T cells during chronic viral infection. PNAS. 2011;108:21182-7.

103. Becattini S., Latorre D., Mele F., Foglierini M., Gregorio C. D., Cassotta A., et al. Functional heterogeneity of human memory CD4+ T cell clones primed by pathogens or vaccines. Science. 2015;347:400-6.

Acknowledgement

The completion of this thesis relied on the tremendous support from many important people during my PhD study. First and foremost, I would like to express my greatest and deepest gratitude to my supervisor Prof. Dirk Busch and also Dr. Veit Buchholz for their guidance throughout the research. The intense discussions we had and the valuable suggestions they gave have all motivated me immensely during the course of this study and also helped me to bring this project into a clearer picture. I would also like to extend the appreciation to Prof. Percy Knolle, Prof. Thomas Korn and Dr. Admar Verschoor for the criticism and intellectual exchange on this project to make it better. In addition, a special thanks to Dr. Michael Flossdorf and Prof. Thomas Höfer who brought the bio-mathematical modeling approach into this study and helped us gain an in-depth insight on the single $CD4^+$ T cell behavior.

Many thanks to Dr. Christian Stemberger and Dr. Veit Buchholz for initiation of the adoptive single T cell transfer approach on $CD8^+$ T cells. It provides me an informative introduction for this project. Furthermore, owing to the fact that most of the works was frequently in need of congenic matrix mice and T cell sorts. I would like to extend my appreciation to Katherine Molter and Inge Hensel for their maintenance of the mouse breeding, as well as Dr. Matthias Schiemann, Lynette Henkel and Immanuel Andrä for their assistance in the FACS sorts. Of course, a big thanks also goes to all of my colleagues in AG Busch for the intensive discussion and technical support for my research. It has been a great experience working in this research group with full of nice and friendly ambience that helped me quickly adapt to this new environment. Additionally, I would like to thank Kristoft Wing and Katherine Molter for the critical comment on my thesis.

During the course of my PhD life, I would like to extend my appreciation to my friend Wilson Chang, who has spent a lot of time with me at leisure. Also, I would like to especially thank Shwetha Lakshmipathi and Lynette Henkel because we have shared our lives on both work and personal level. We encouraged each other when we faced the rough times and many other occasions. To me, they are part of my family and it is a great pleasure to have them in my life.

Last but not least, I want to give my deepest gratitude to my family and Yi-Ching, who have been supporting me and loving me unconditionally. Without their encouragement and selfless support, I would not be able to pursue my study.